Supplementary Information

Activating circularly polarized luminescence through environment-modulated polymorphic assembly of glycerolipid-modified carbazolyl phthalonitriles

Chuanqing Lan,[a] Xiao Chen,[a] Qingshuang Zou,[a] Zhiqi Liu,[b] Liwen Jiang,[b] Zhifeng Huang[a] and Dennis K. P. Ng*[a]

---

[a] Department of Chemistry, The Chinese University of Hong Kong, Shatin, N.T., Hong Kong, China. E-mail: dkpn@cuhk.edu.hk

[b] School of Life Sciences, The Chinese University of Hong Kong, Shatin, N.T., Hong Kong, China

Contents

Experimental Section

General

N,*N*-Dimethylformamide (DMF) was purified using an INERT solvent purification system. All other solvents and reagents were of reagent grade and used as received. All the reactions were performed under an atmosphere of nitrogen and monitored by thin layer chromatography (TLC) performed on Merck pre-coated silica gel 60 F254 plates. Chromatographic purification was performed with column chromatography on silica gel (Macherey-Nagel, 230-400 mesh).

^{1}H, $^{13}C\{^{1}H\}$, and $^{19}F\{^{1}H\}$ NMR spectra were recorded on a Bruker Avance III 400 spectrometer (^{1}H, 400 MHz; ^{13}C, 101 MHz; ^{19}F, 376 MHz) or a Bruker Avance III 500 spectrometer (^{1}H, 500 MHz; ^{13}C, 126 MHz; ^{19}F, 470 MHz) in $CDCl_3$. ^{1}H and $^{13}C\{^{1}H\}$ NMR spectra were referenced internally by using the residual solvent (^{1}H: $\delta = 7.26$) or solvent (^{13}C: $\delta = 77.2$) resonance(s) relative to tetramethylsilane. For $^{19}F\{^{1}H\}$ NMR spectra, trifluoromethylbenzene (δ = -64 ppm) was used as the external reference. High-resolution electrospray ionization (ESI) mass spectra were recorded on a Thermo Scientific Q Exactive Focus Orbitrap mass spectrometer. UV-Vis, circular dichroism (CD), and photoluminescence (PL) spectra, as well as circularly polarized luminescence (CPL) were recorded using an Applied Photophysics Chirascan V100+ CD spectrometer. The absorption asymmetry factor g_{CD} was determined using the equation: g_{CD} = CD(mdeg)/32982A, using the CD intensity and absorbance (A).[R1] Fluorescence lifetime measurements by time-correlated single photon counting were conducted using a HORIBA FluoroMax Plus spectrofluorometer equipped with a 330 nm nanosecond pulsed diode laser. Raman spectra were recorded on a Renishaw inVia Qontor spectrometer system. Dynamic light scattering (DLS) was performed on a Malvern Panalytical Zetasizer Nano ZS90 system. Atomic force microscopy (AFM) images were captured on a Bruker NanoWizard 4 XP Bioscience atomic force microscope. Optical rotation was recorded on a Autopol® II automatic polarimeter at 589 nm (Na D-Line) with a light path

length of 100 mm. Chiral analysis for (*R*)- and (*S*)-**9** was performed by Daicel Chiral Technologies (China) Co., Ltd.

Preparation of (*S*)-3

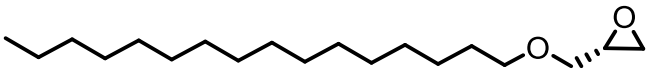

According to the previously described procedure,[R2] cetyl alcohol (6.0 g, 25 mmol), NaOH (1.6 g, 75 mmol), and tetrabutylammonium bromide (TBAB) (0.37 g, 1.25 mmol) were added into hexane (20 mL) with stirring. (*R*)-(-)-Epichlorohydrin (ee = 94-100%) (Aladdin Scientific Corp.) (4.0 mL, 50 mmol) was then added into this mixture, followed by heating under reflex for 5 h. After naturally cooling to room temperature, the mixture was filtered, and the filtrate was rotary-evaporated to give (*S*)-**3** as a white solid (7.4 g, 99%). $[\alpha]_D$ +6.00° (5.0 g in 100 mL of benzene), giving an ee value of 62% by making reference to the $[\alpha]_D$ values of optically pure (*S*)-(+)-**3** (+10.00°) and (*R*)-(-)-**3** (-9.83°) reported previously.[R3] ^{1}H NMR (400 MHz, $CDCl_3$): δ 3.71 (dd, *J* = 11.6, 3.2 Hz, 1 H, OCH), 3.45-3.52 (m, 2 H, OCH_2), 3.38 (dd, *J* = 11.6, 6.0 Hz, 1 H, OCH), 3.13-3.17 (m, 1 H, OCH), 2.80 (virtual t, *J* = 4.8 Hz, 1 H, OCH), 2.61 (dd, *J* = 4.8, 2.8 Hz, 1 H, OCH), 1.59 (quintet, *J* = 7.2 Hz, 2 H, CH_2), 1.20-1.38 (m, 28 H, CH_2), 0.88 (t, *J* = 6.8 Hz, 3 H, CH_3).

Preparation of (*R*)-3

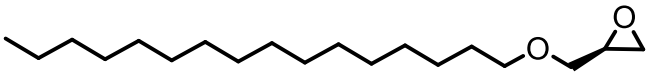

According to the above procedure using (*S*)-(+)-epichlorohydrin (ee = 73-82%) (Aladdin Scientific Corp.) instead of the (*R*)-isomer as starting material, (*R*)-**3** was obtained as a white

solid (7.1 g, 95%). $[\alpha]_D$ -6.12° (5.0 g in 100 mL of benzene), giving an ee value of 64% as described above. ^{1}H NMR (500 MHz, $CDCl_3$): δ 3.70 (dd, *J* = 11.5, 3.0 Hz, 1 H, OCH), 3.45-3.52 (m, 2 H, OCH_2), 3.38 (dd, *J* = 11.5, 5.5 Hz, 1 H, OCH), 3.14-3.16 (m, 1 H, OCH), 2.80 (virtual t, *J* = 5.0 Hz, 1 H, OCH), 2.61 (dd, *J* = 5.0, 3.0 Hz, 1 H, OCH), 1.59 (quintet, *J* = 7.0 Hz, 2 H, CH_2), 1.20-1.36 (m, 28 H), 0.88 (t, *J* = 7.0 Hz, 3 H, CH_3).

Preparation of (*R*)-5

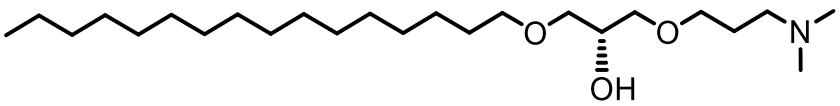

3-Dimethylamino-1-propanol (**4**) (2.5 mL, 22 mmol) and 18-crown-6 (0.7 g, 2.6 mmol) were dissolved in diglyme (20 mL) and then potassium (0.8 g, 22 mmol) was added to deprotonate the alcohol. After complete consumption of the potassium, a solution of (*S*)-**3** (3.13 g, 10.5 mmol) in diglyme (10 mL) was added. The mixture was then stirred at 80 °C overnight. After that, it was poured into a saturated NH_4Cl solution (50 mL). The mixture was extracted with CH_2Cl_2 (20 mL × 3). The combined organic layer was dried over anhydrous Na_2SO_4 and then evaporated to dryness under reduced pressure. The residue was purified by column chromatography on silica gel using $CHCl_3$ followed by $CHCl_3$/MeOH (5:1) as eluents to give (*R*)-**5** (2.94 g, 66%). ^{1}H NMR (400 MHz, $CDCl_3$): δ 3.94-4.00 (m, 1 H, OCH), 3.67-371 (m, 2 H, OCH_2), 3.54-3.63 (m, 2 H, OCH_2), 3.41-3.47 (m, 4 H, OCH_2), 3.21 (t, *J* = 7.2 Hz, 2 H, NCH_2), 2.86 (s, 6 H, NCH_3), 2.12 (quintet, *J* = 6.8 Hz, 2 H, CH_2), 1.56 (quintet, *J* = 6.8 Hz, 2 H, CH_2), 1.26 (br s, 26 H, CH_2), 0.88 (t, *J* = 6.4 Hz, CH_3). $^{13}C\{^1H\}$ NMR (126 MHz, $CDCl_3$): δ 72.6, 71.8, 71.7, 69.2, 68.2, 65.9, 56.6, 43.5, 43.3, 31.9, 29.7, 29.6, 29.5, 29.4, 26.1, 24.8, 22.7, 14.2 (some of the signals are overlapped). HRMS (ESI): *m*/*z* calcd for $C_{24}H_{52}NO_3^+$ $[M+H]^+$, 402.3950; found, 402.3938.

Preparation of (*S*)-5

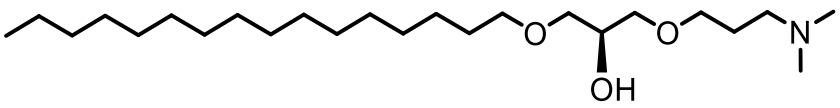

According to the above procedure using (*R*)-**3** instead of (*S*)-**3** as starting material, (*S*)-**5** was obtained (2.31 g, 52%). ^{1}H NMR (500 MHz, $CDCl_3$): δ 3.96-4.00 (m, 1 H, OCH), 3.69-376 (m, 2 H, OCH_2), 3.55-3.65 (m, 2 H, OCH_2), 3.43-3.45 (m, 4 H, OCH_2), 3.24 (t, *J* = 7.0 Hz, 2 H, NCH_2), 2.88 (s, 6 H, NCH_3), 2.11 (quintet, *J* = 6.5 Hz, 2 H, CH_2), 1.55 (quintet, *J* = 6.5 Hz, 2 H, CH_2), 1.26 (br s, 26 H, CH_2), 0.88 (t, *J* = 7.0 Hz, CH_3). ^{13}C{^{1}H} NMR (126 MHz, $CDCl_3$): δ 72.3, 71.9, 71.7, 70.6, 69.5, 69.4, 56.6, 45.1, 31.9, 29.7, 29.6, 29.5, 29.4, 27.2, 26.1, 22.7, 14.1 (some of the signals are overlapped). HRMS (ESI): *m*/*z* calcd for $C_{24}H_{52}NO_3^+$ $[M+H]^+$, 402.3950; found, 402.3944.

Preparation of (*R*)-7

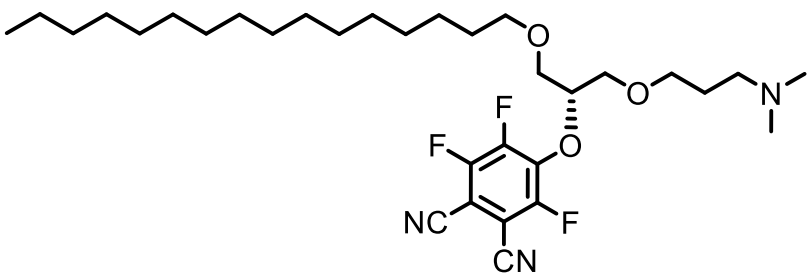

A mixture of (*R*)-**5** (1 g, 2.5 mmol), tetrafluorophthalonitrile (**6**) (0.8 g, 4.0 mmol), and K_2CO_3 (0.37 g, 3.33 mmol) in DMF (15 mL) was stirred at room temperature overnight. The mixture was then poured into water (30 mL), and the resulting mixture was extracted with Et_2O (20 mL × 3). The combined organic layer was dried over anhydrous Na_2SO_4 and then evaporated to dryness under reduced pressure. The residue was purified by column chromatography on silica gel using $CHCl_3$ followed by $CHCl_3$/MeOH (20:1) as eluents to give (*R*)-**7** (0.51 g, 35%). ^{1}H

NMR (400 MHz, $CDCl_3$): δ 4.74-4.79 (m, 1 H, OCH), 3.65-3.75 (m, 4 H, OCH_2), 3.45-3.50 (m, 2 H, OCH_2), 3.37-3.42 (m, 2 H, OCH_2), 2.22-2.27 (m, 8 H, NCH_2 and NCH_3), 1.63-1.67 (m, 2 H, CH_2), 1.45 (quintet, J = 6.8 Hz, 2 H, CH_2), 1.26 (br s, 26 H, CH_2), 0.88 (t, J = 6.8 Hz, 3 H, CH_3). $^{13}C\{^1H\}$ NMR (126 MHz, $CDCl_3$): δ 154.2 (ddd, J = 262.1, 5.0, 2.5 Hz), 150.0 (ddd, J = 255.8, 15.1, 2.5 Hz), 147.8 (ddd, J = 257.0, 13.9, 5.0 Hz), 143.2 (ddd, J = 13.9, 10.1, 5.0 Hz), 109.2 (dt, J = 11.3, 2.5 Hz), 100.0 (dt, J = 17.6, 3.8 Hz), 97.9 (dt, J = 16.4, 2.5 Hz), 84.5 (t, J = 2.5 Hz), 71.9, 70.8, 70.0, 56.3, 45.4, 31.9, 29.7, 29.6, 29.5, 29.4, 29.3, 27.8, 26.0, 22.7, 14.1 (some of the signals are overlapped). $^{19}F\{^1H\}$ NMR (470 MHz, $CDCl_3$): δ -119.0 (dd, J = 14.1, 9.4 Hz), -128.3 (dd, J = 18.8, 9.4 Hz), -136.0 (dd, J = 18.8, 14.1 Hz). HRMS (ESI): *m*/*z* calcd for $C_{32}H_{51}F_3N_3O_3^+$ $[M+H]^+$, 582.3885; found, 582.3864.

Preparation of (*S*)-7

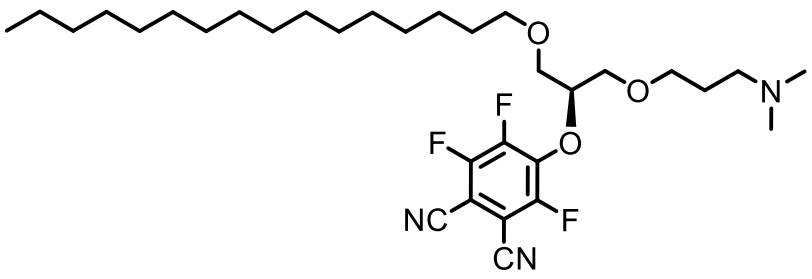

According to the above procedure using (*S*)-**5** instead of (*R*)-**5** as starting material, (*S*)-**7** was obtained (0.36 g, 25%). ^1H NMR (500 MHz, $CDCl_3$): δ 4.74-4.79 (m, 1 H, OCH), 3.65-3.73 (m, 4 H, OCH_2), 3.45-3.50 (m, 2 H, OCH_2), 3.37-3.43 (m, 2 H, OCH_2), 2.24 (t, J = 6.5 Hz, 2 H, NCH_2), 2.21 (s, 6 H, NCH_3), 1.66 (quintet, J = 8.5 Hz, 2 H, CH_2), 1.45 (quintet, J = 7.0 Hz, 2 H, CH_2), 1.26 (br s, 26 H, CH_2), 0.88 (t, J = 7.0 Hz, 3 H, CH_3). $^{13}C\{^1H\}$ NMR (126 MHz, $CDCl_3$): δ 154.2 (ddd, J = 262.1, 5.0, 2.5 Hz), 150.0 (ddd, J = 257.0, 15.1, 2.5 Hz), 148.0 (ddd, J = 259.6, 13.9, 6.3 Hz), 143.2 (ddd, J = 13.9, 11.3, 2.5 Hz), 109.3 (dt, J = 11.3, 2.5 Hz), 100.0 (dt, J = 18.9, 3.8 Hz), 98.0 (dt, J = 16.4, 2.5 Hz), 84.5 (t, J = 2.5 Hz), 72.0, 70.8, 70.0, 56.3,

45.4, 31.9, 29.7, 29.6, 29.5, 29.4, 27.8, 26.0, 22.7, 14.1 (some of the signals are overlapped). $^{19}F\{^{1}H\}$ NMR (376 MHz, $CDCl_3$): δ -118.9 (dd, J = 13.5, 9.4 Hz), -128.4 (dd, J = 20.7, 9.4 Hz), -136.0 (dd, J = 20.7, 13.5 Hz). HRMS (ESI): m/z calcd for $C_{32}H_{51}F_3N_3O_3^+$ $[M+H]^+$, 582.3885; found, 582.3889.

Preparation of (*R*)-9

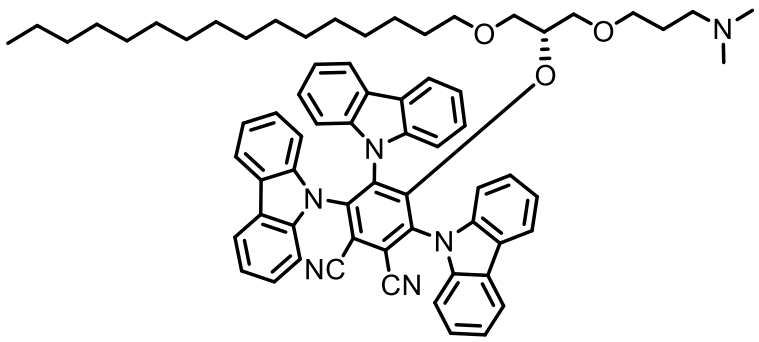

A mixture of (*R*)-**7** (0.25 g, 0.43 mmol), carbazole (**8**) (0.29 g, 1.76 mmol), and K_2CO_3 (0.4 g, 3.52 mmol) in DMF (2 mL) was stirred at room temperature for 3 days. After that, the mixture was poured into water (20 mL), and the resulting mixture was extracted with Et_2O (20 mL × 3). The combined organic layer was dried over anhydrous Na_2SO_4 and then evaporated to dryness under reduced pressure. The residue was purified repeatedly by column chromatography on silica gel first using acetonitrile, MeOH, acetone, and $CHCl_3$/MeOH (20:1) sequentially as the eluents. Finally, the crude product was further recrystallized from hexane and chloroform to give (*R*)-**9** (0.27 g, 62%) with an ee value of 91% determined by chiral HPLC. ^1H NMR (500 MHz, $CDCl_3$): δ 8.19 (d, J = 9.5 Hz, 2 H, Ar-H), 7.60-7.73 (m, 6 H, Ar-H), 7.41-7.49 (m, 4 H, Ar-H), 6.98-7.09 (m, 12 H, Ar-H), 3.14-3.16 (m, 1 H, OCH), 2.44-2.61 (m, 6 H, OCH_2), 2.25-2.39 (m, 10 H, OCH_2, NCH_2, and NCH_3), 1.27-1.31 (m, 26 H, CH_2), 1.16-1.19 (m, 2 H CH_2), 1.03-1.08 (m, 2 H CH_2), 0.88 (t, J = 8.5 Hz, 3 H, CH_3). HRMS (ESI): m/z calcd for $C_{68}H_{75}N_6O_3^+$ $[M+H]^+$, 1023.5906; found, 1023.5873.

Preparation of (*S*)-9

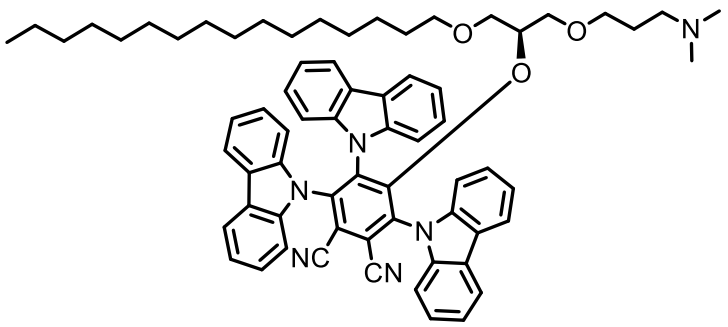

According to the above procedure using (*S*)-**7** instead of (*R*)-**7** as starting material, (*S*)-**9** was obtained (0.30 g, 68%). The ee value was determined to be 94% by chiral HPLC. ^{1}H NMR (500 MHz, $CDCl_3$): δ 8.20 (d, J = 9.5 Hz, 2 H, Ar-H), 7.61-7.73 (m, 6 H, Ar-H), 7.43-7.51 (m, 4 H, Ar-H), 6.99-7.13 (m, 12 H, Ar-H), 3.14-3.16 (m, 1 H, OCH), 2.56-2.69 (m, 4 H, OCH_2), 2.50-2.53 (m, 2 H, OCH_2), 2.45 (br s, 6 H, NCH_3), 2.24-2.32 (m 4 H, OCH_2 and NCH_2), 1.28 (br s, 28 H, CH_2), 1.09-1.11 (m, 2 H CH_2), 0.89 (t, J = 8.5 Hz, 3 H, CH_3). HRMS (ESI): *m*/*z* calcd for $C_{68}H_{75}N_6O_3^+$ $[M+H]^+$, 1023.5906; found, 1023.5903.

Preparation of Chiral Lipid Nanotubes

The Cz_3PN-lipid nanotubes were prepared using a Havard Apparatus PHD 2000 syringe pump and a microfluidic Y-shaped mixer (Anhui Chixin Biotechnology Co., Ltd.),[R4] similar to that for preparing general lipid nanoparticles.[R5] The channel parameters of the microfluidic chip are given in Fig. S7. Briefly, an ethanol solution of optical pure Cz_3PN-lipid (100 μM) was injected through the alcohol channel at a flow rate of 100 μL min^{-1}, while citrate buffer (50 mM, pH 4.0) was injected through the aqueous channel at a flow rate of 500 μL min^{-1} at room temperature. Most of the alcohol in the resulting mixture was then removed by a rotary evaporator to give the nanotubes.

Preparation of Lipid Nanocones on a Glass Surface

Microscope slide cover glass (Propper Manufacturing Co., Inc.) was immersed in a piranha solution [i.e., a mixture of sulfuric acid and 30% hydrogen peroxide, 3:1 (v/v)] at 50-60 °C overnight. The glass coverslips were then washed with deionized water and dried at room temperature before being coated with optical pure Cz_3PN-lipid by dipping into its solution in ethanol (1 mM, 30 μL), followed by natural drying.

Preparation of Lipid Nanohemispheres on a PDMS Surface

A solution of optical pure Cz_3PN-lipid in ethanol (1 mM, 30 μL) was dropped on a PDMS surface (Hangzhou Westru Technology Co., Ltd.). After drying naturally, a film of lipid nanohemispheres was obtained.

Cryo-Transmission Electron Microscopic Study

Quantifoil R1.2/1.3 Cu 300 mesh grids were glow discharged at 30 mA for 30 s with a holding time of 5 s (PELCO, easiGlow, Ted Pella). For each type of Cz_3PN-modified glycerolipid nanotubes [(*R*) and (*S*)-**9**], 3 μL of 20 μM of the dispersion was applied on the front side of the glow-discharged grid and blotted for 1.5 s with 0 force and 5 s drain time for two times before plunge freezing (Mark IV Vitrobot, Thermo Fisher Scientific). Sample application and blotting was conducted at 22 ℃ and 100% humidity in the chamber of the Vitrobot. Samples were imaged under a cryo-transmission electron microscope (Talos F200C, Thermo Fisher Scientific) using a Ceta-D CCD camera (Thermo Fisher Scientific) at 73,000× (pixel size = 0.20 nm).

Measurement of CD and CPL Spectra

Liquid samples were placed in a four-side transparent cuvette. For CD spectroscopic measurements, the incident and emitted light beams were in the same direction, and a blank solvent was used for background correction. For CPL measurements, the incident and emitted

light beams were aligned perpendicularly. For thin-film samples, the film was perpendicular to the incident light in CD measurements. To eliminate linear polarization, four measurements at 0°, 90°, 180°, and 270° were taken, and the average value was recorded. A blank glass or PDMS slide was used for background correction. For CPL measurements, the incident light and the film were oriented at an angle of 45°. To eliminate linear polarization, four measurements at 0°, 90°, 180°, and 270° were taken, and the average value was recorded.

References

R1 P. Xi, W. Zhao, Y. Cao, S. Xie, P. Wang, G. Ungar, X. Ye and F. Liu, *Small*, 2025, **21**, 2408176.

R2 M. Zhou, G. Luo, Z. Zhang, S. Li and C. Wang, *J. Mol. Struct.*, 2017, **1144**, 199-205.

R3 S. D. Stamatov and J. Stawinski, *Org. Biomol. Chem.*, 2007, **5**, 3787-3800.

R4 A. D. Stroock, S. K. W. Dertinger, A. Ajdari, I. Mezić, H. A. Stone and G. M. Whitesides, *Science*, 2002, **295**, 647-651.

R5 C. B. Roces, G. Lou, N. Jain, S. Abraham, A. Thomas, G. W. Halbert and Y. Perrie, *Pharmaceutics*, 2020, **12**, 1095.

(a)

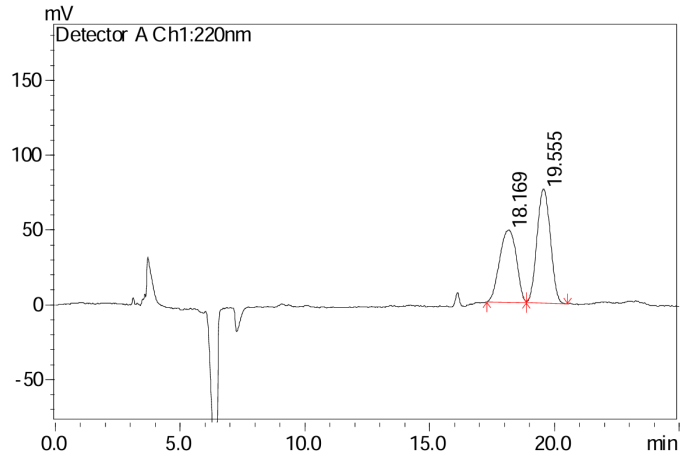

(b)

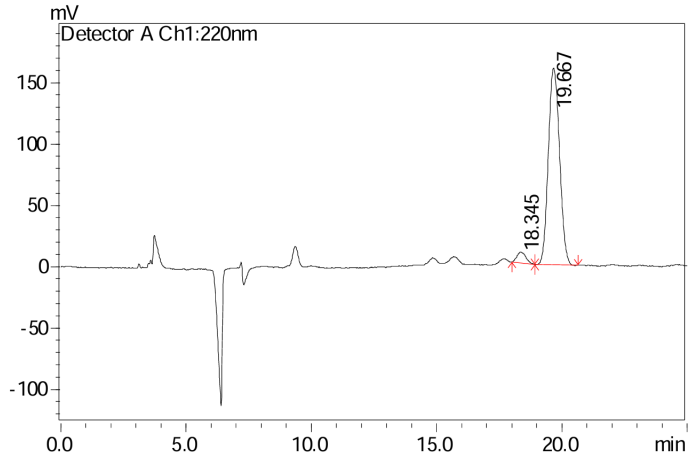

(c)

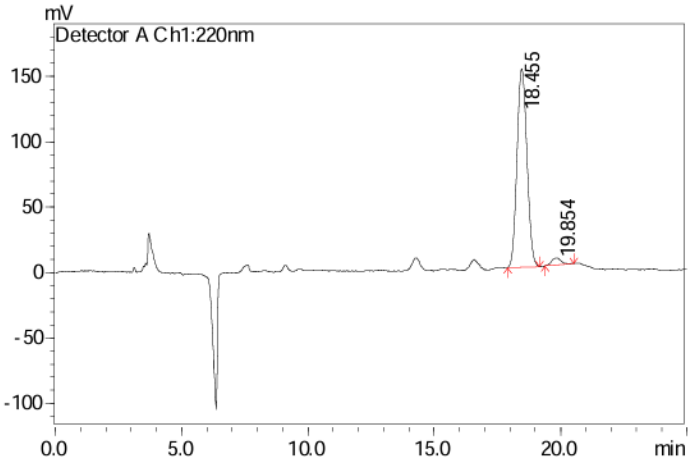

Fig. S1 Chromatograms of (a) a mixture of (*R*) and (*S*)-**9**, (b) (*R*)-**9**, and (c) (*S*)-**9**.

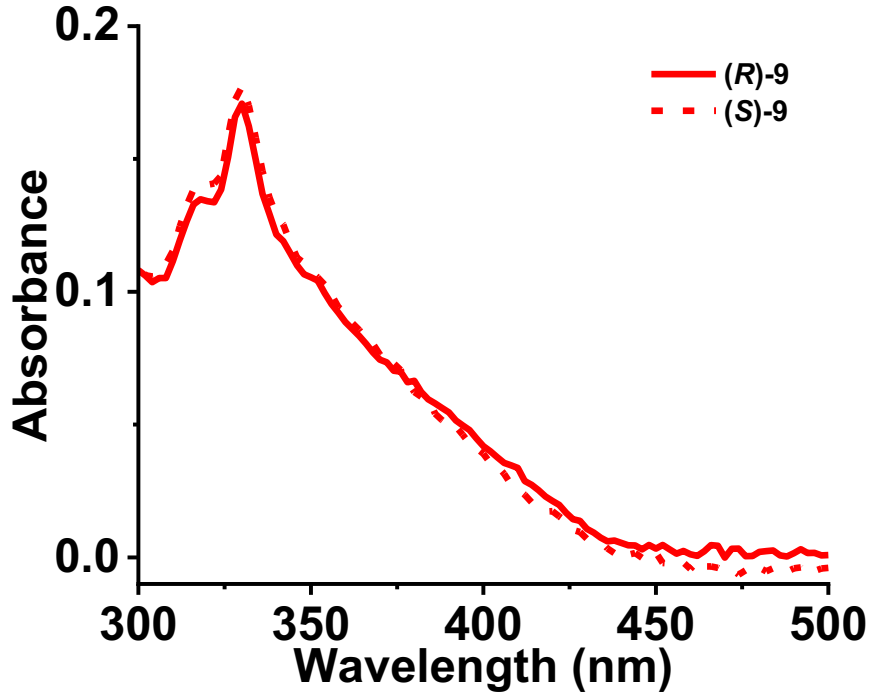

Fig. S2 Electronic absorption spectra of (*R*) and (*S*)-**9** in DMF (20 μM).

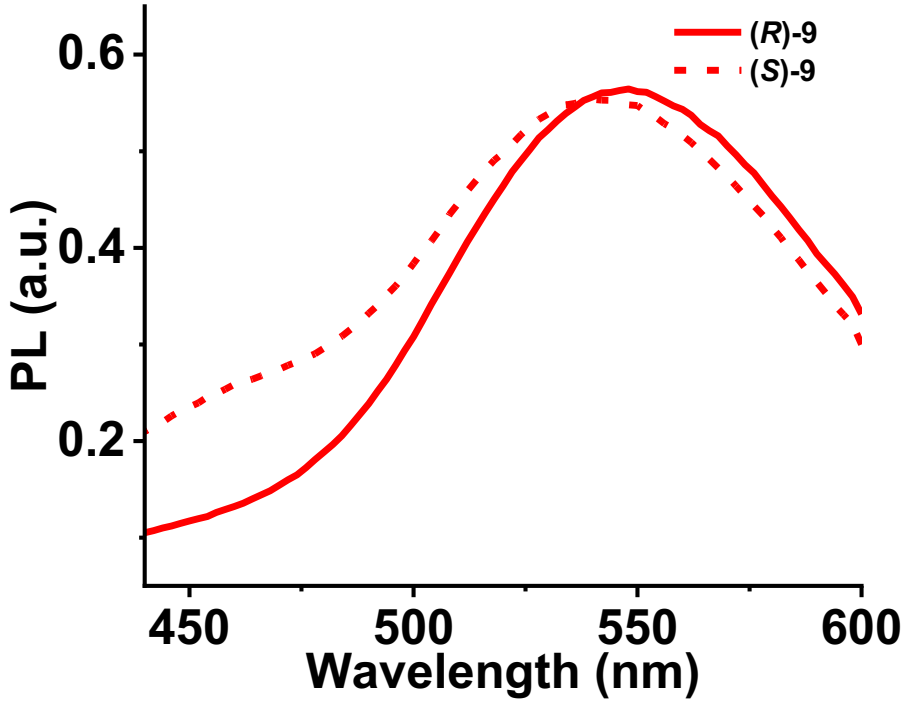

Fig. S3 Fluorescence spectra of (*R*) and (*S*)-**9** in DMF (20 μM) (λ_{ex} = 320 nm).

(a)

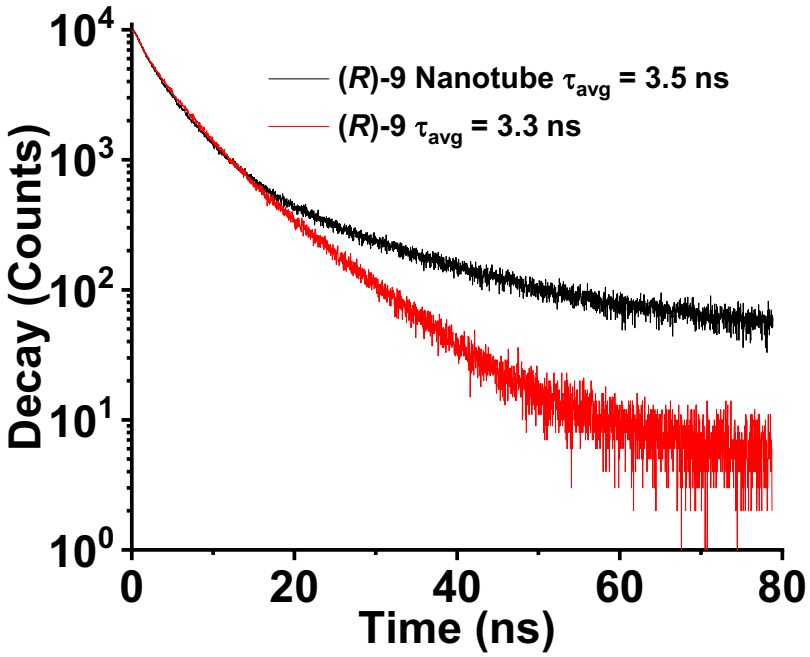

(b)

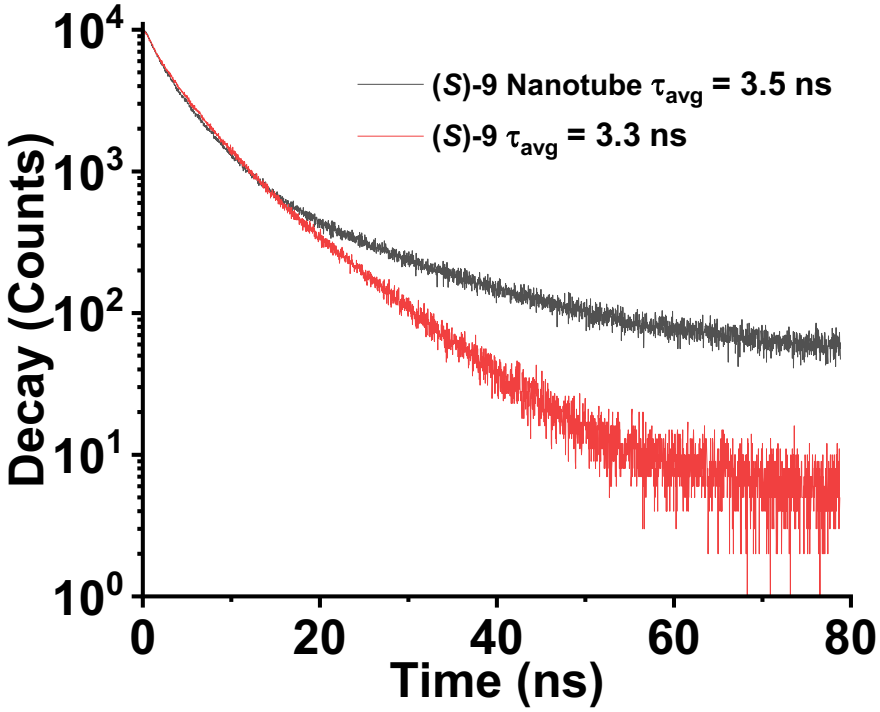

Fig. S4 Fluorescence decay of (a) (*R*)-**9** in DMF and citrate buffer (50 mM, pH 4.0) and (b) (*S*)-**9** in DMF and citrate buffer (50 mM, pH 4.0) with excitation using a 330 nm nanosecond pulsed diode laser and monitoring at 525 nm.

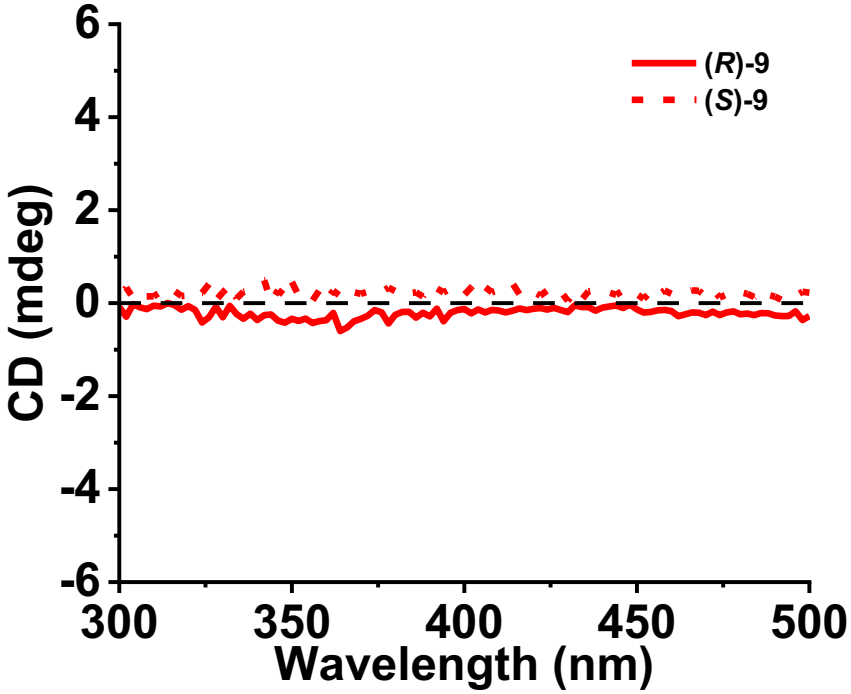

Fig. S5 CD spectra of (*R*) and (*S*)-**9** in DMF (20 μM).

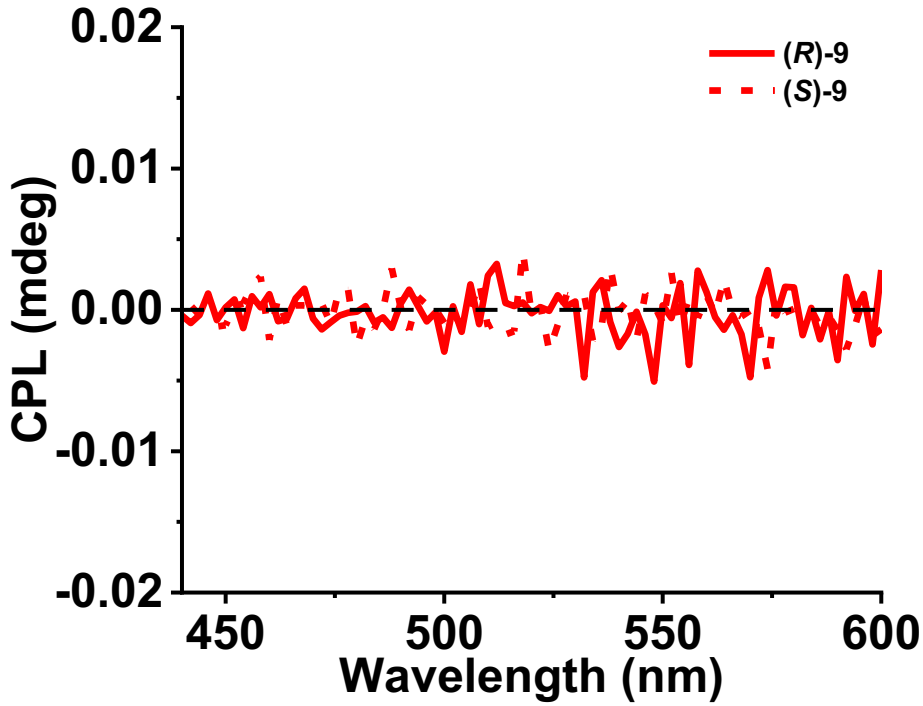

Fig. S6 CPL spectra of (*R*) and (*S*)-**9** in DMF (20 μM).

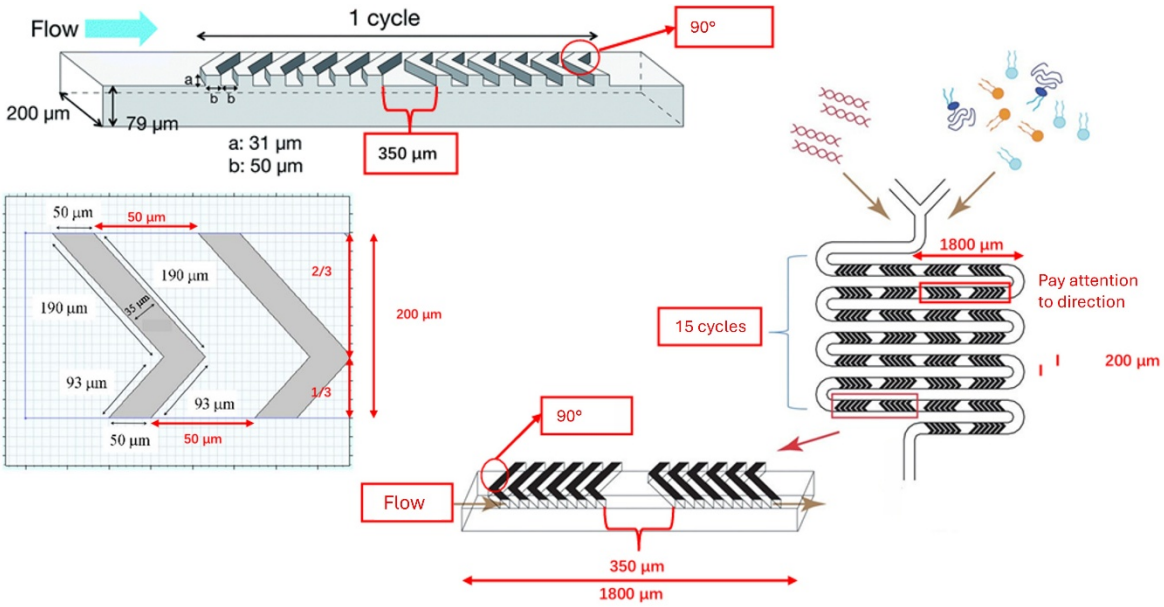

Fig. S7 Channel parameter diagram of the microfluidic Y-shape chip provided by the manufacturer (Anhui Chixin Biotechnology Co., Ltd.).

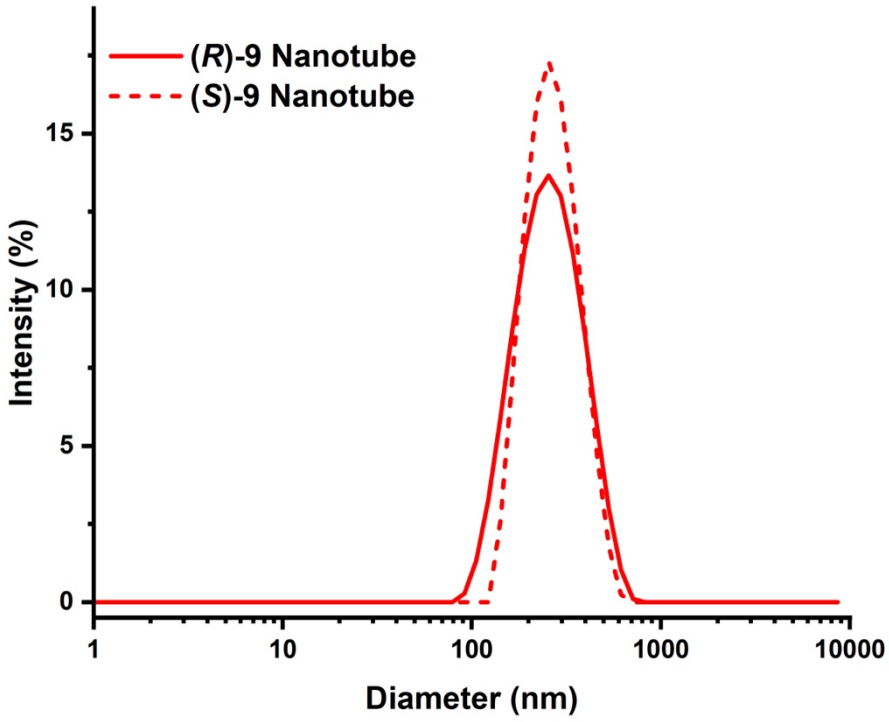

Fig. S8 Hydrodynamic diameter distribution of the nanoparticles formed by nanoprecipitation of Cz_3PN-modified glycerolipids (*R*) and (*S*)-**9**.

(a)

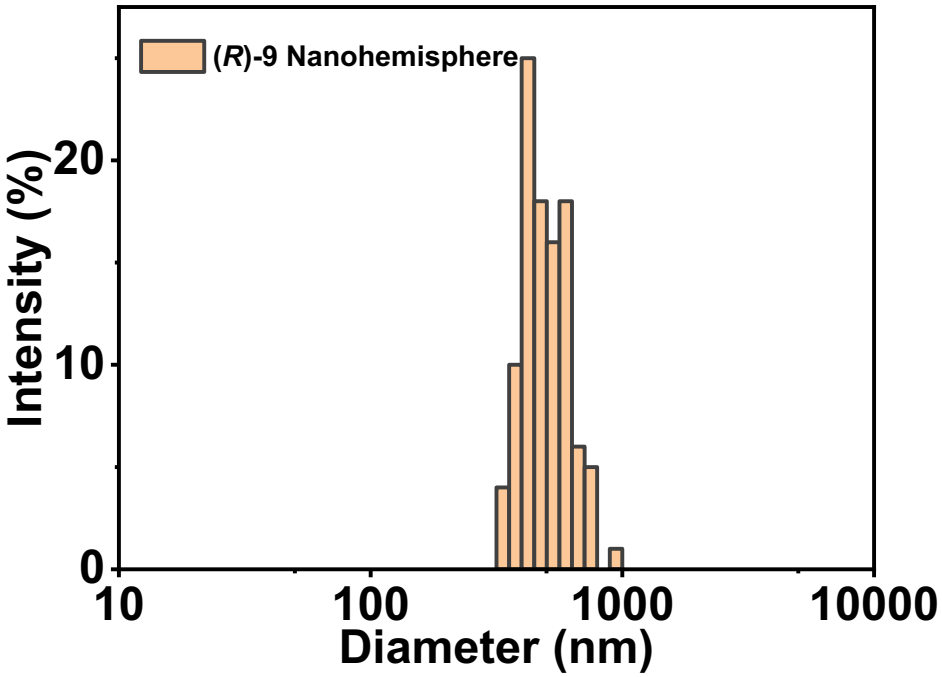

(b)

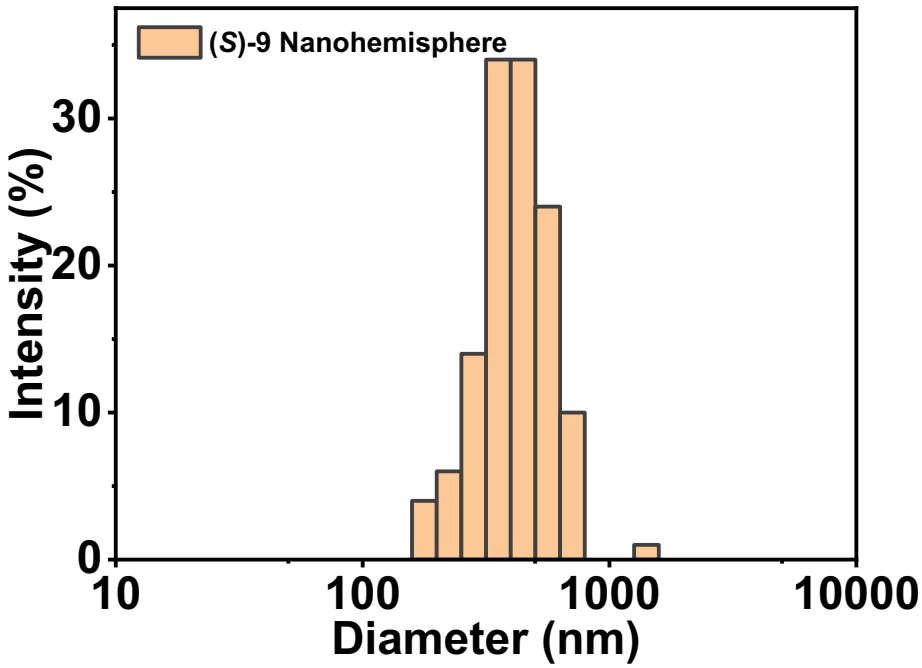

Fig. S9 Statistical analyses of the AFM image of the nanostructures of (a) (*R*)-**9** and (b) (*S*)-**9** formed on PDMS (n = 100-150).

(a)

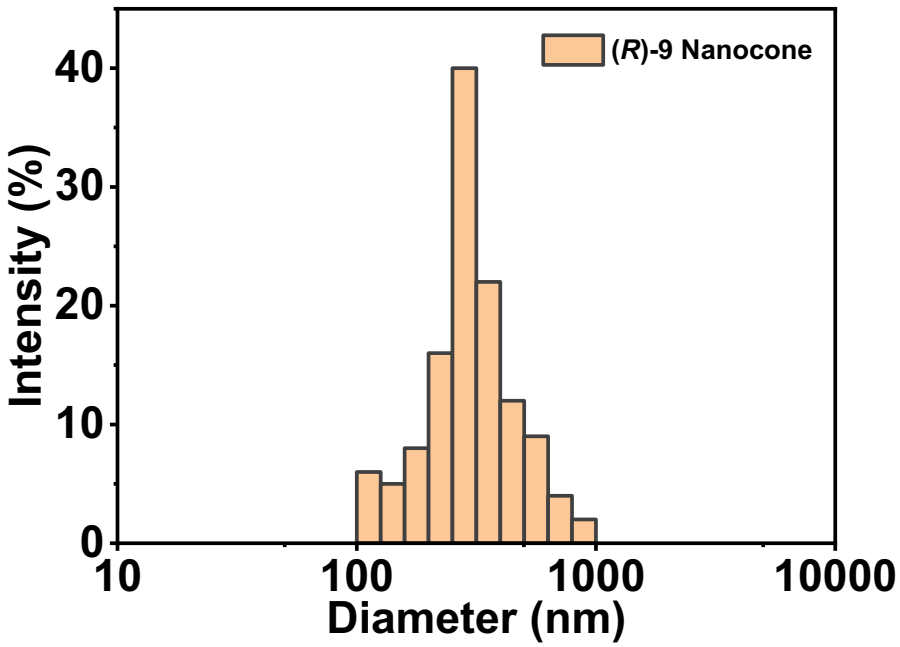

(b)

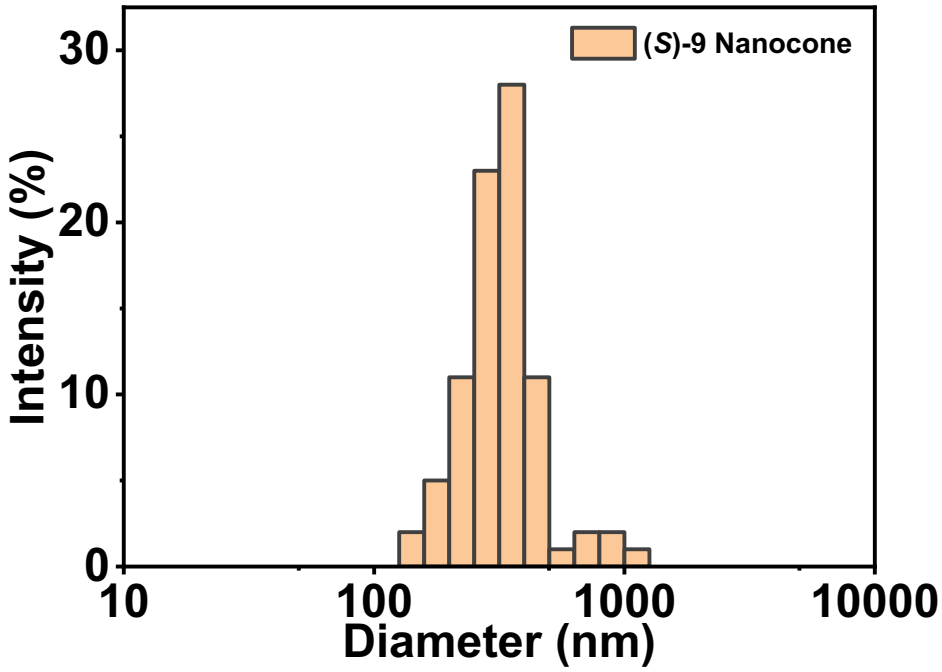

Fig. S10 Statistical analyses of the AFM image of the nanostructures of (a) (*R*)-**9** and (b) (*S*)-**9** formed on glass (n = 100-150).

(a)

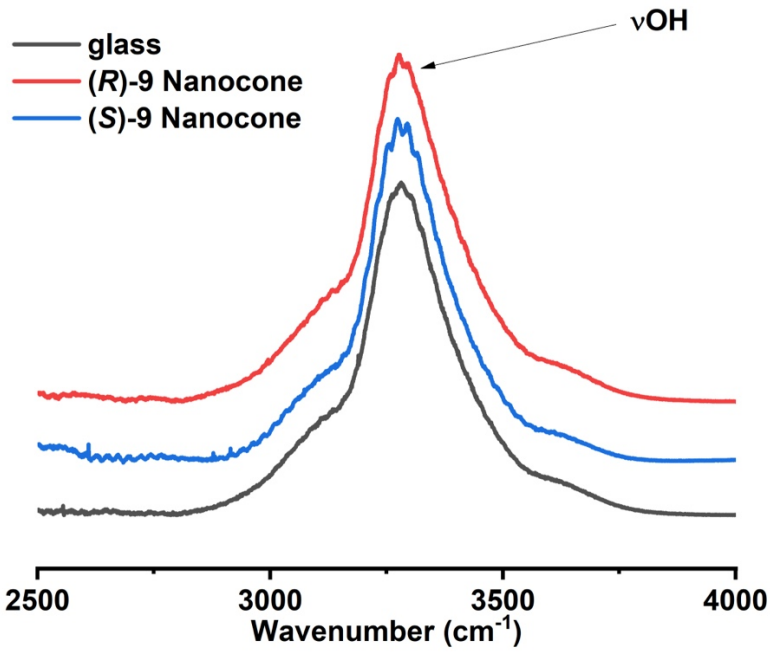

(b)

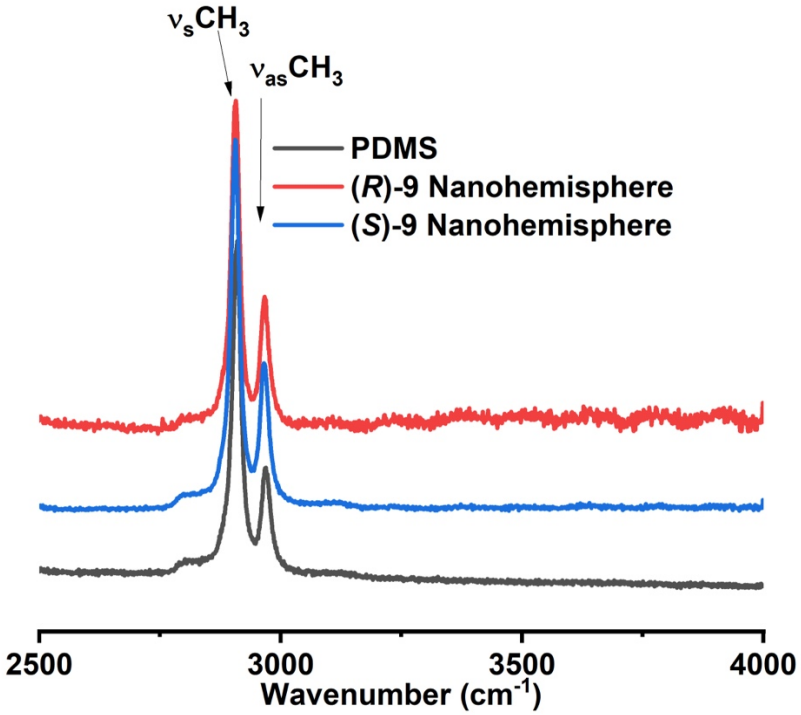

Fig. S11 Raman spectra of (a) the nanocones of (*R*) and (*S*)-**9** formed on glass and (b) the nanohemispheres of (*R*) and (*S*)-**9** formed on PDMS. The spectra of the corresponding neat surfaces are also included for comparison.

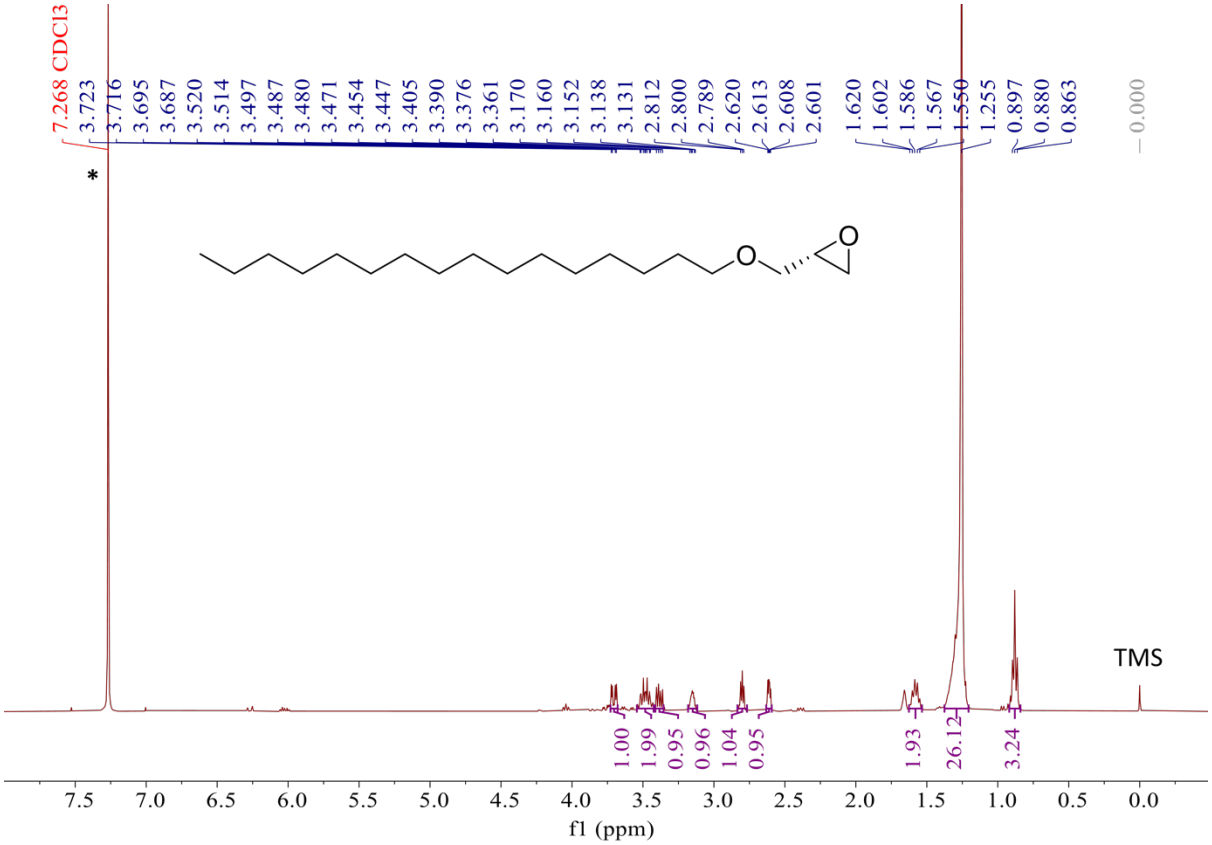

Fig. S12 ^{1}H NMR spectrum of (*S*)-**3** in $CDCl_3$.

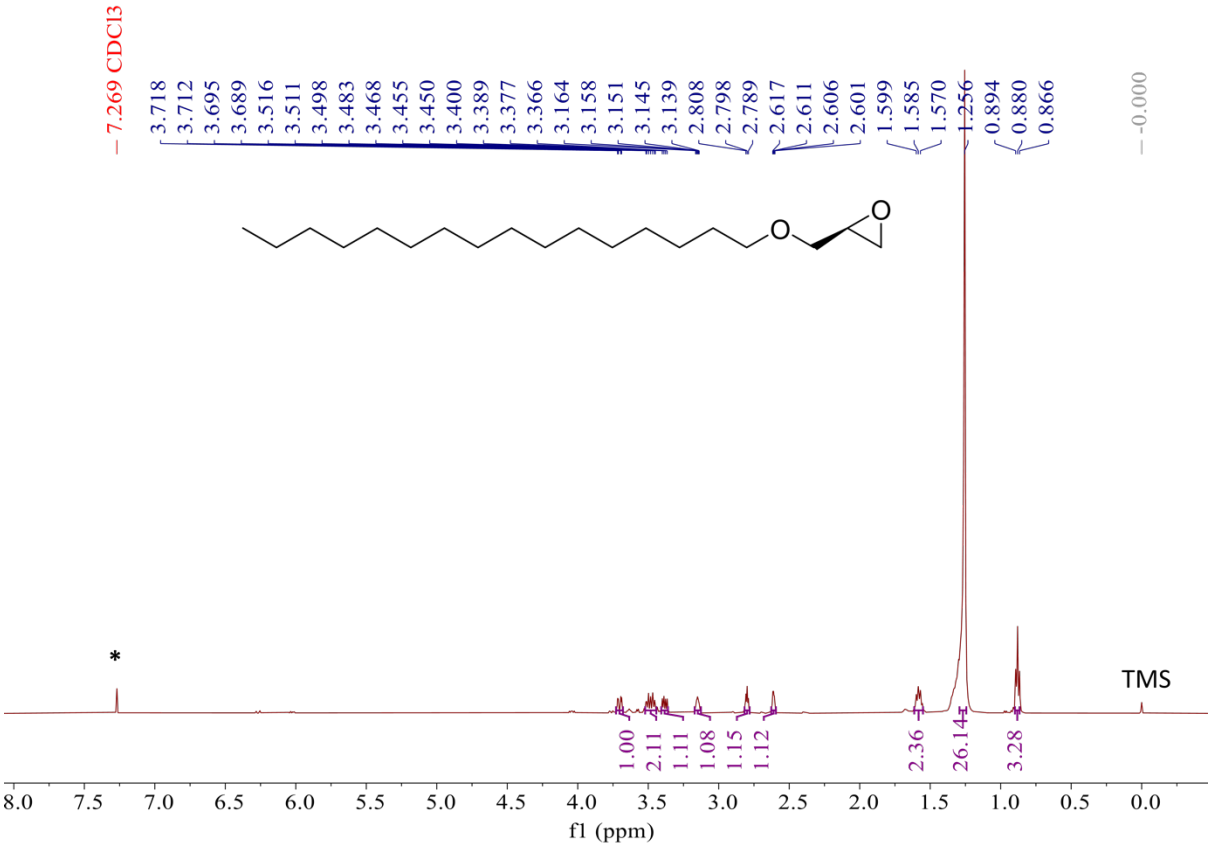

Fig. S13 ^{1}H NMR spectrum of (*R*)-**3** in $CDCl_3$.

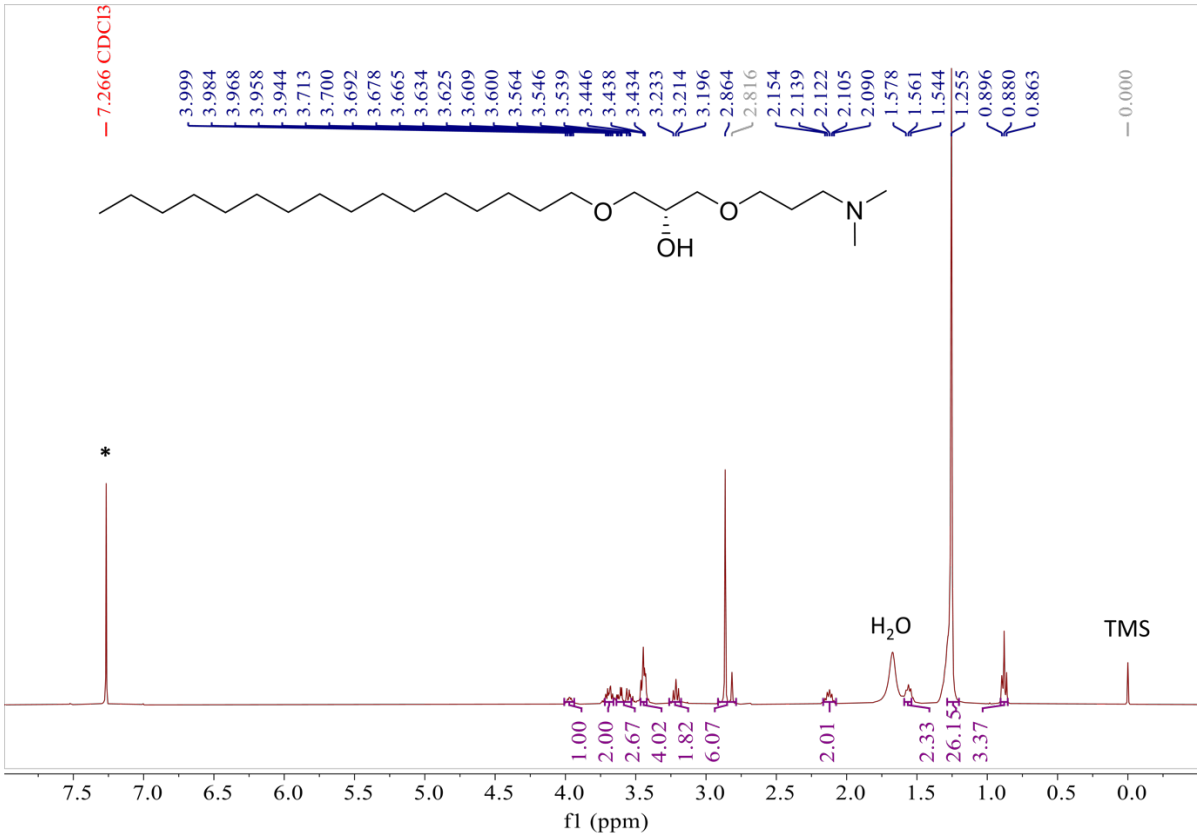

Fig. S14 ^{1}H NMR spectrum of (*R*)-**5** in $CDCl_3$.

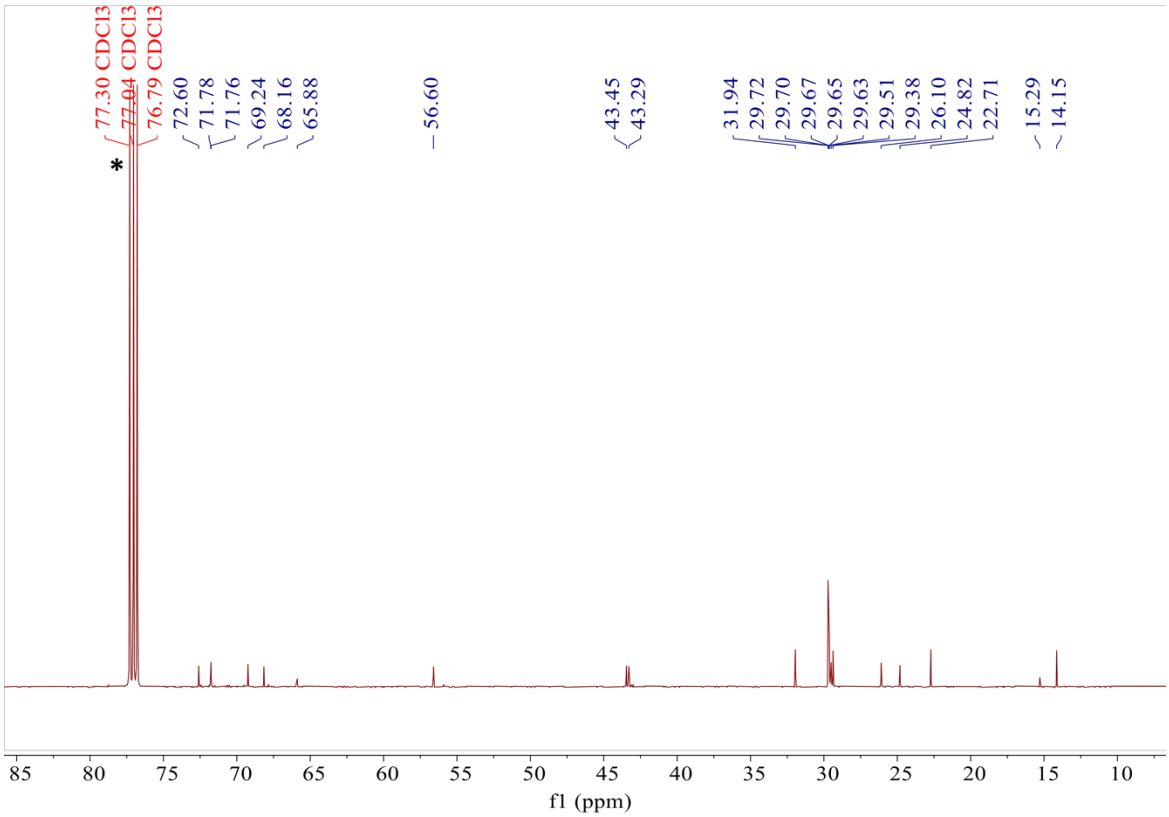

Fig. S15 ^{13}C{^{1}H} NMR spectrum of (*R*)-**5** in $CDCl_3$.

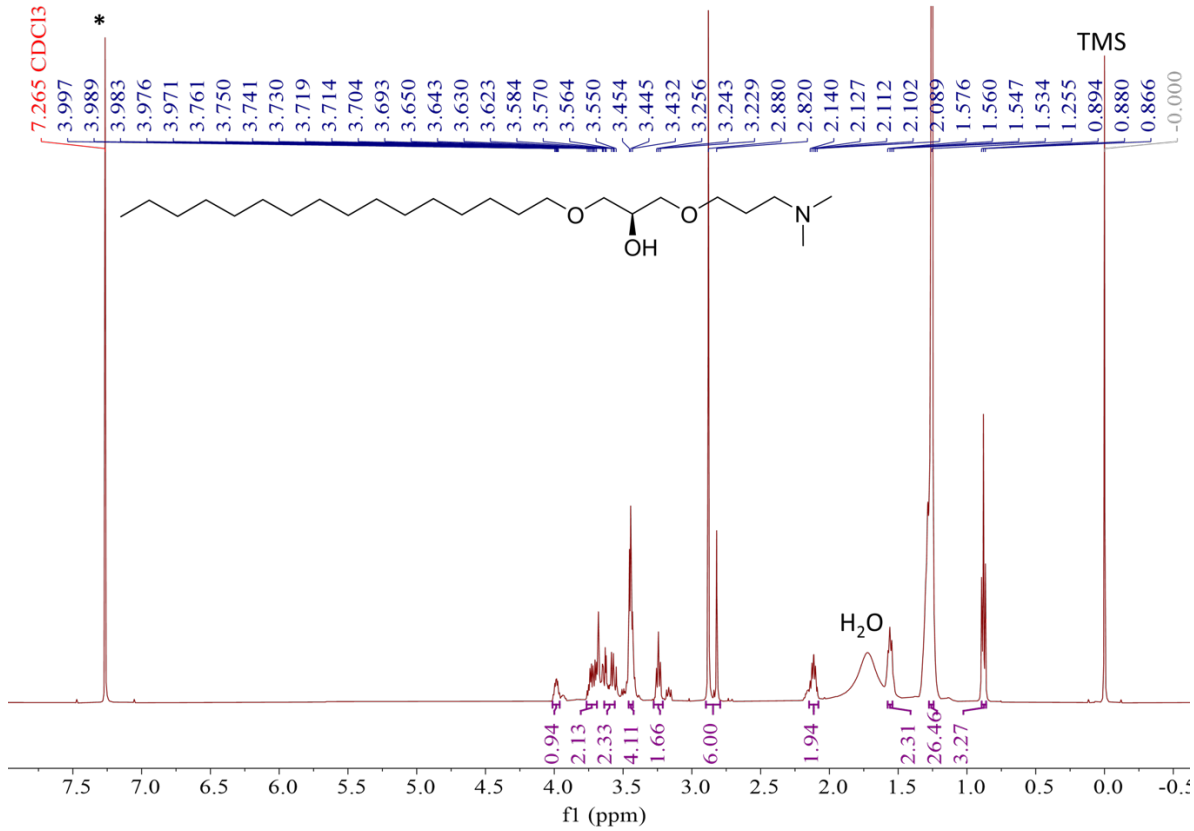

Fig. S16 ^{1}H NMR spectrum of (*S*)-**5** in $CDCl_3$.

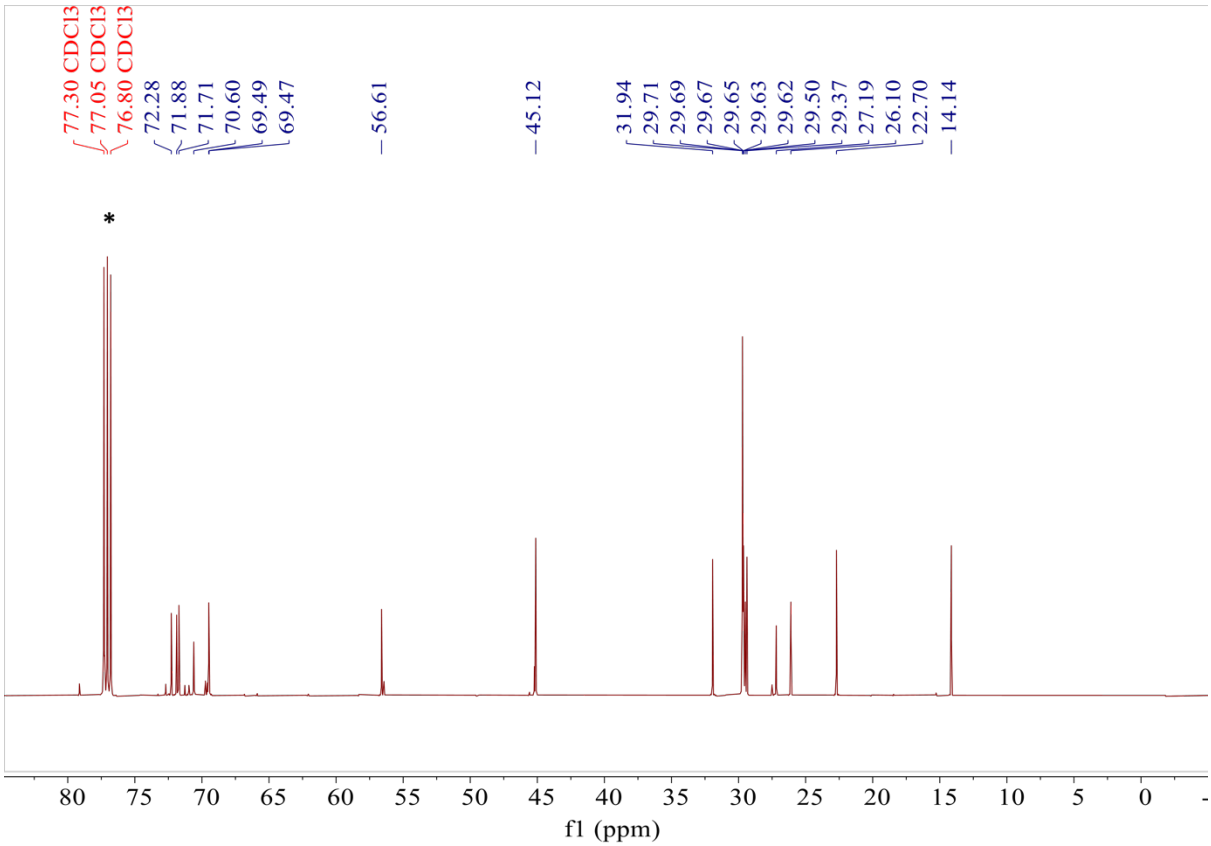

Fig. S17 $^{13}C\{^{1}H\}$ NMR spectrum of (*S*)-**5** in $CDCl_3$.

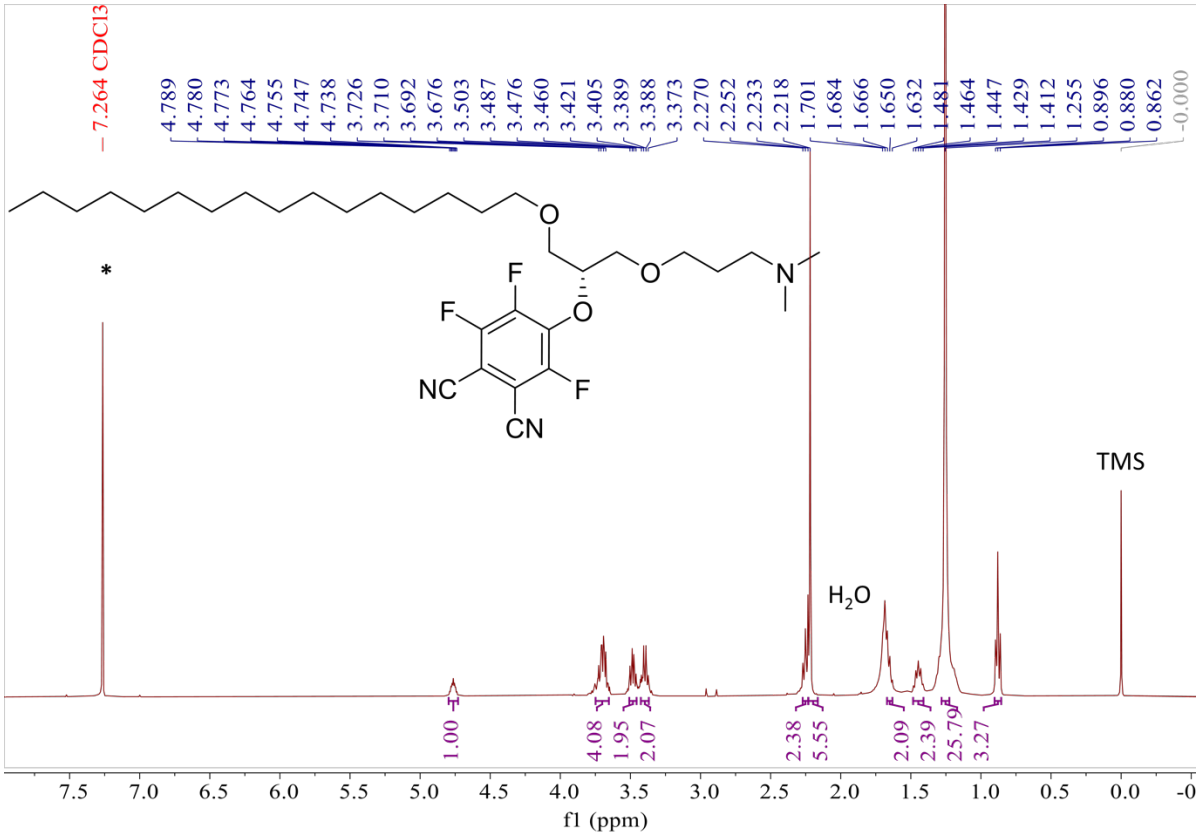

Fig. S18 ^{1}H NMR spectrum of (*R*)-**7** in $CDCl_3$.

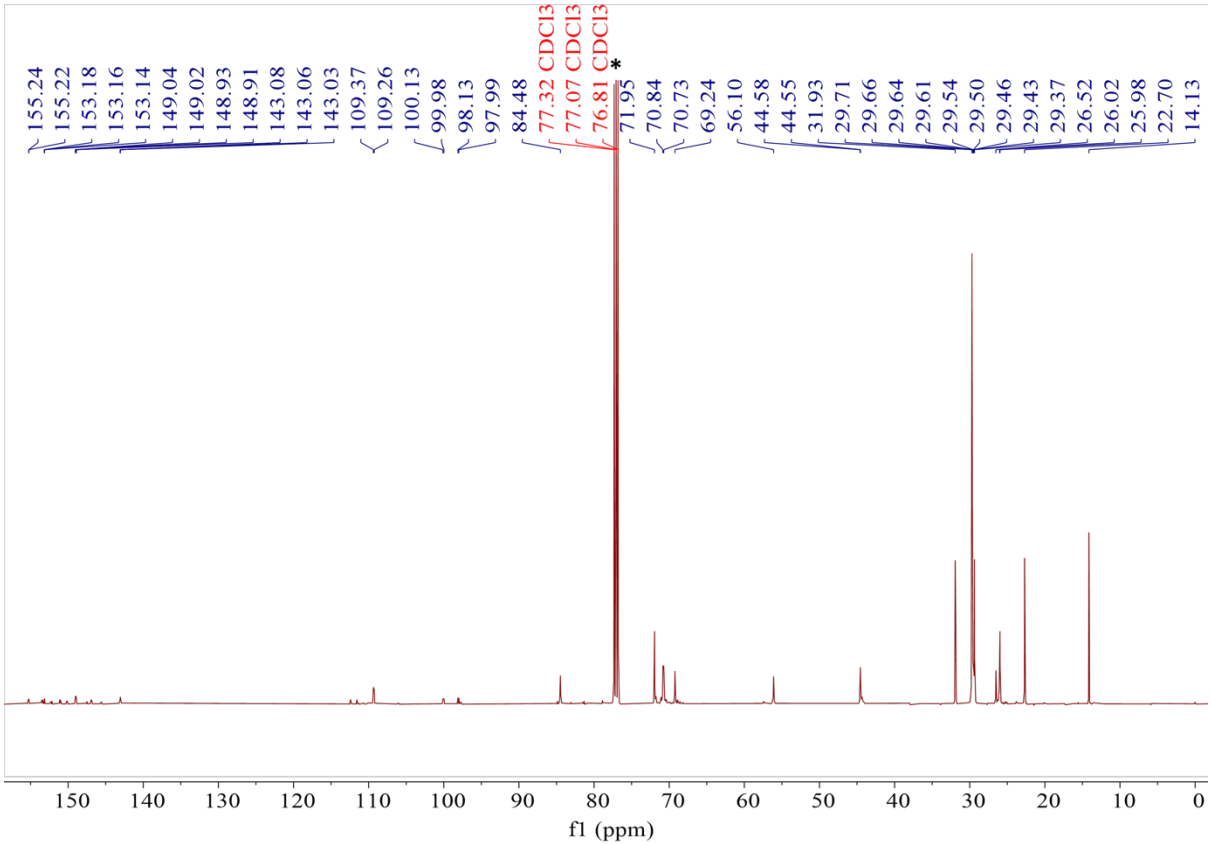

Fig. S19 $^{13}C\{^{1}H\}$ NMR spectrum of (*R*)-**7** in $CDCl_3$.

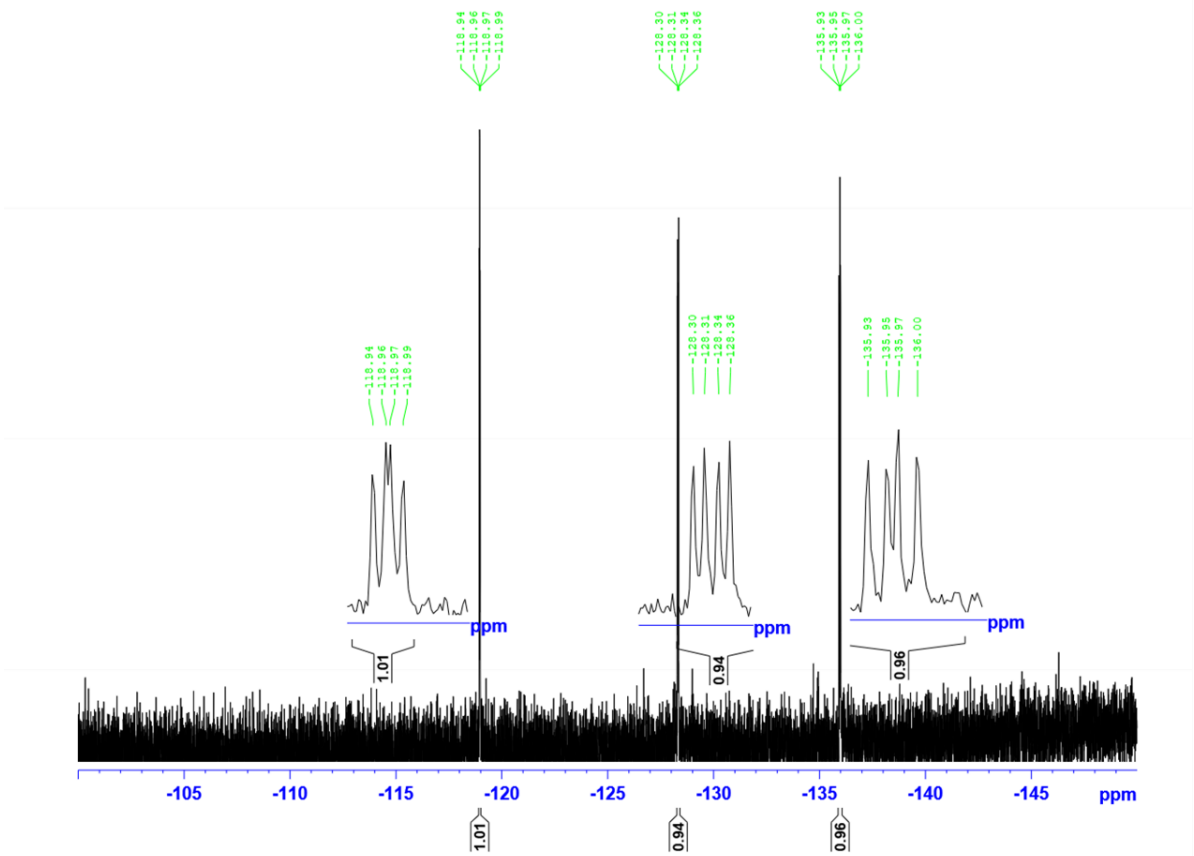

Fig. S20 $^{19}F\{^{1}H\}$ NMR spectrum of (*R*)-**7** in $CDCl_3$.

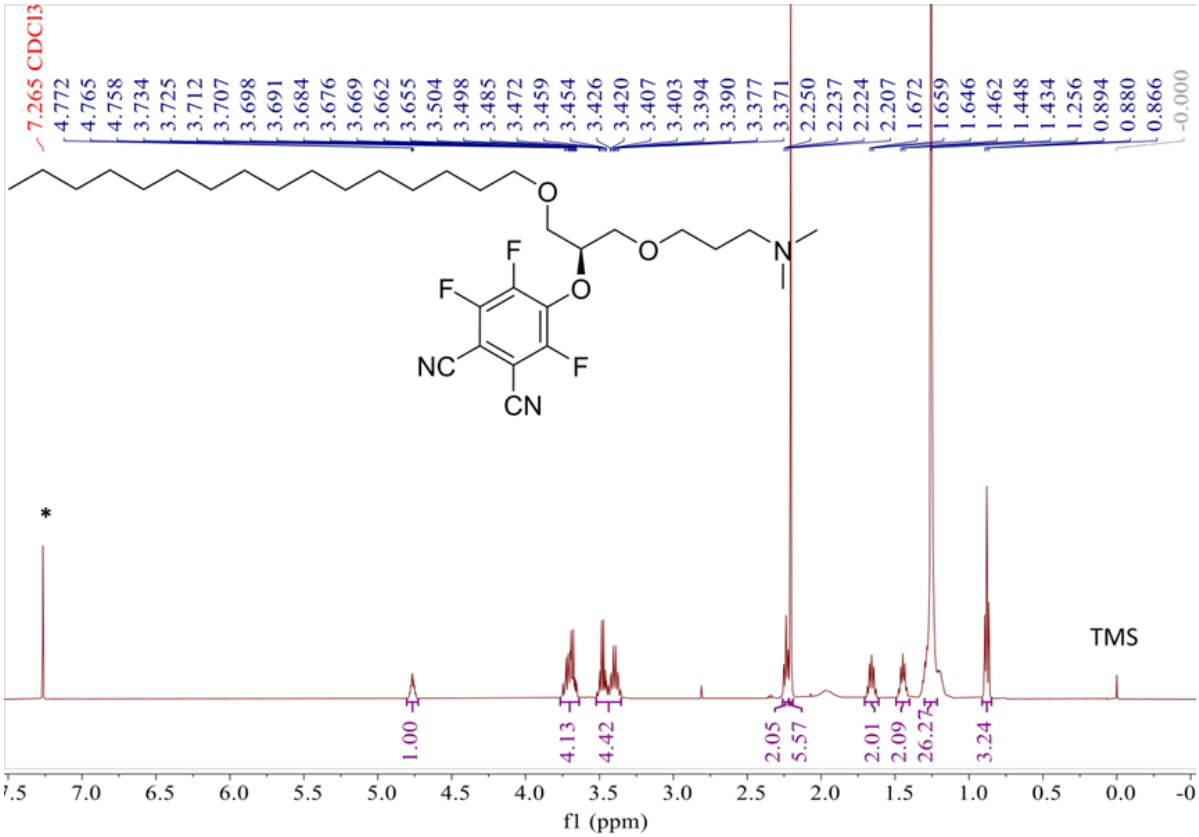

Fig. S21 ^{1}H NMR spectrum of (*S*)-**7** in $CDCl_3$.

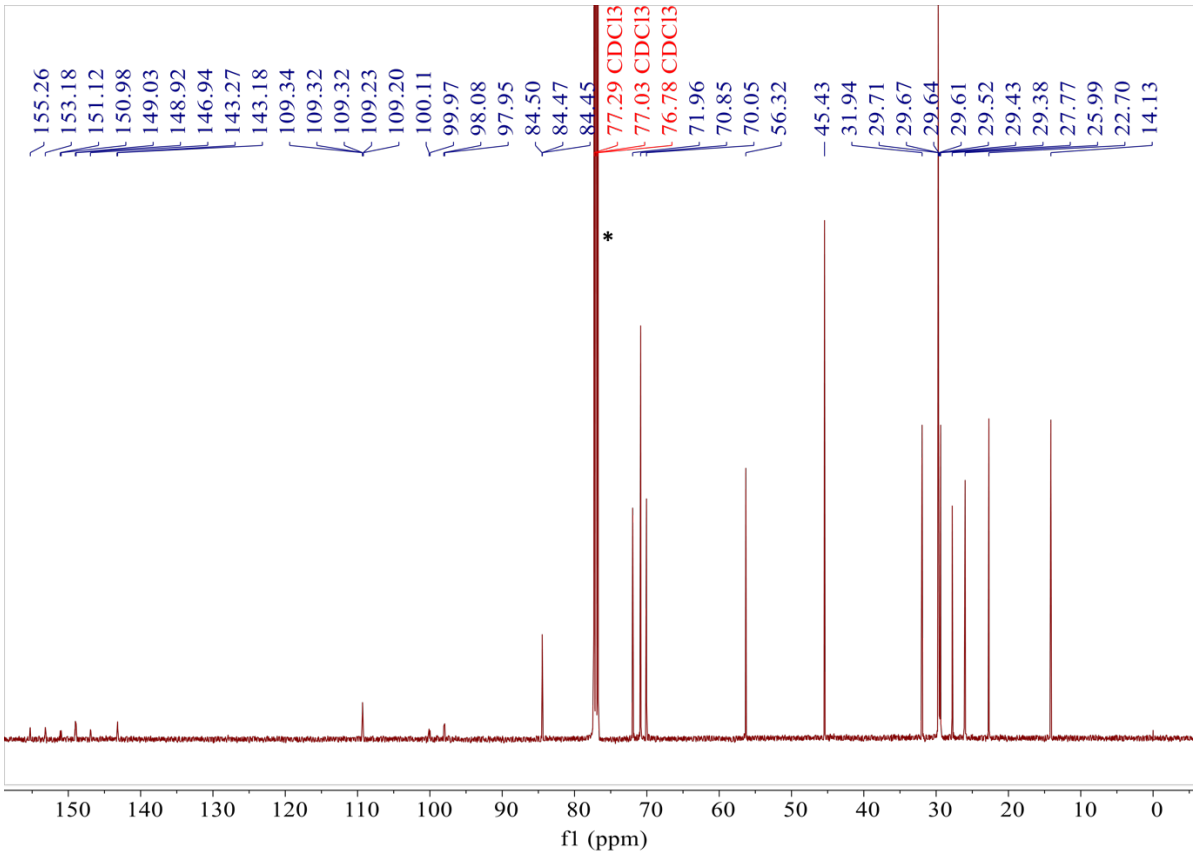

Fig. S22 $^{13}C\{^{1}H\}$ NMR spectrum of (*S*)-**7** in $CDCl_3$.

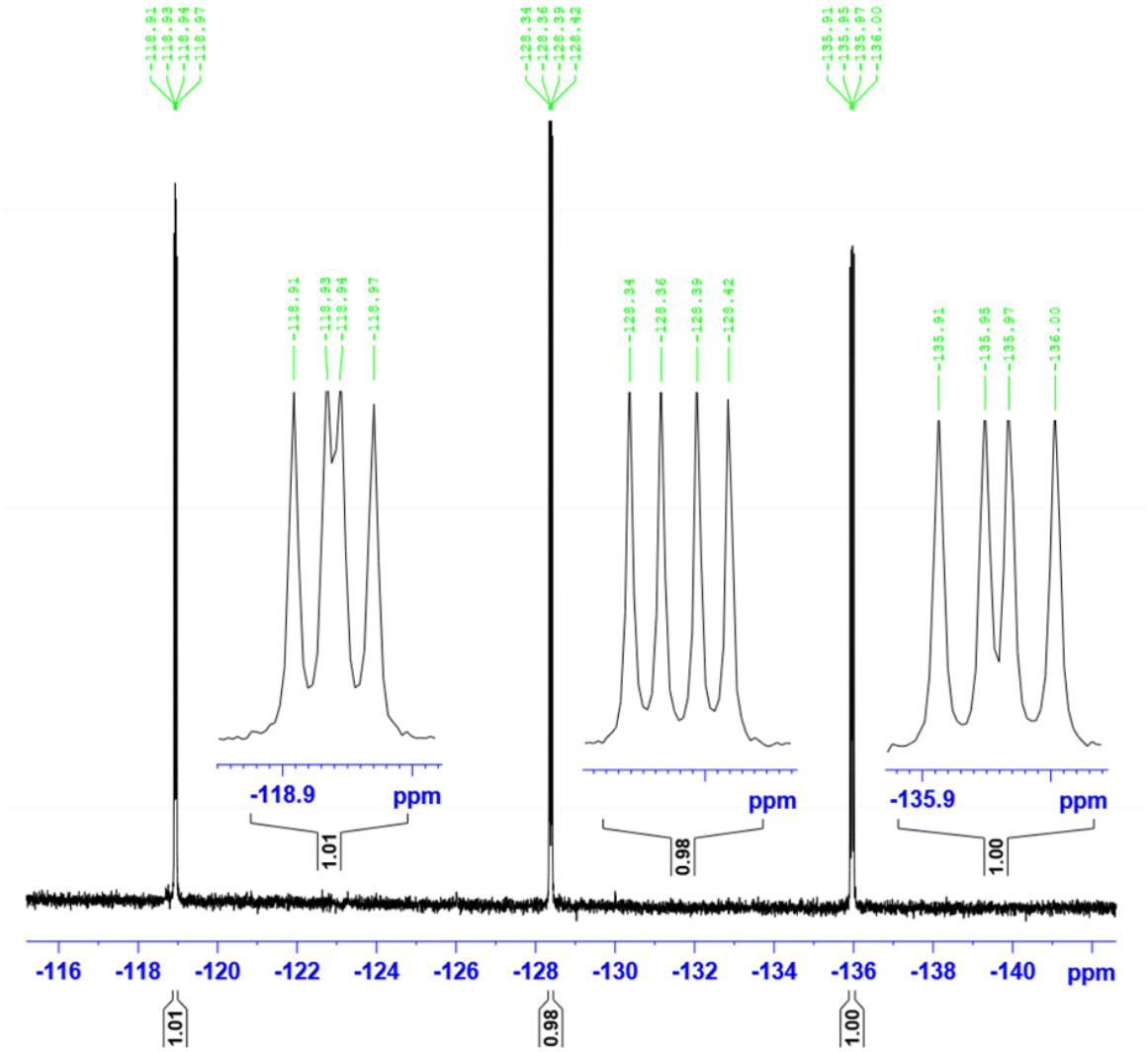

Fig. S23 $^{19}F\{^{1}H\}$ NMR spectrum of (*S*)-**7** in $CDCl_3$.

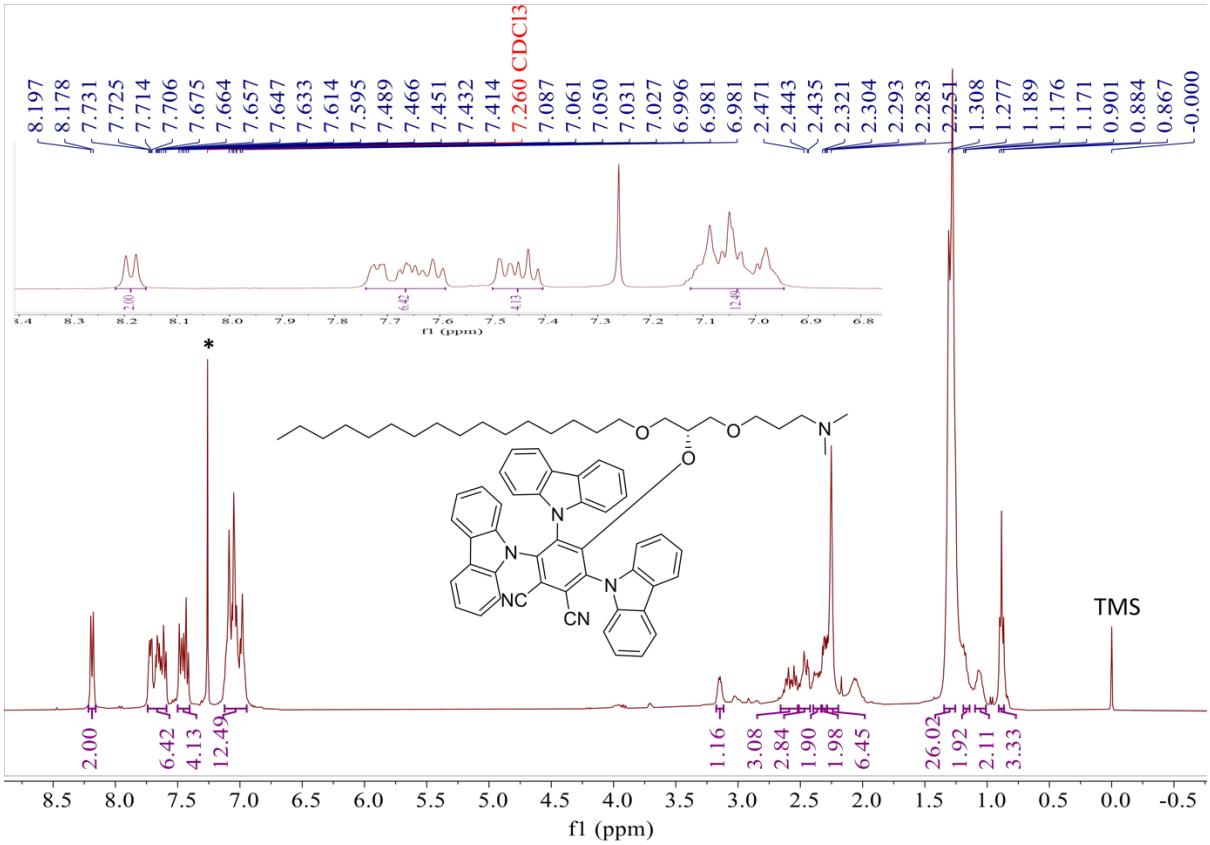

Fig. S24 ^{1}H NMR spectrum of (*R*)-**9** in $CDCl_3$.

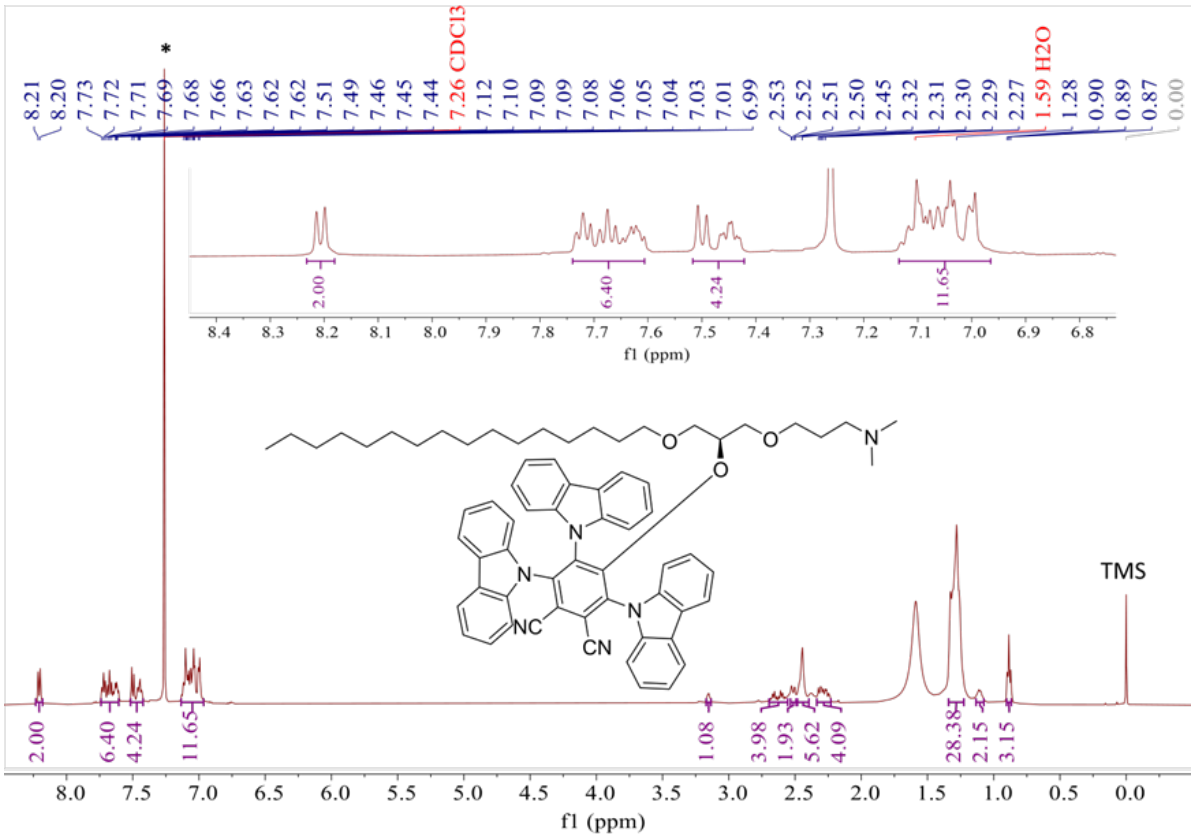

Fig. S25 ^{1}H NMR spectrum of (*S*)-**9** in $CDCl_3$.

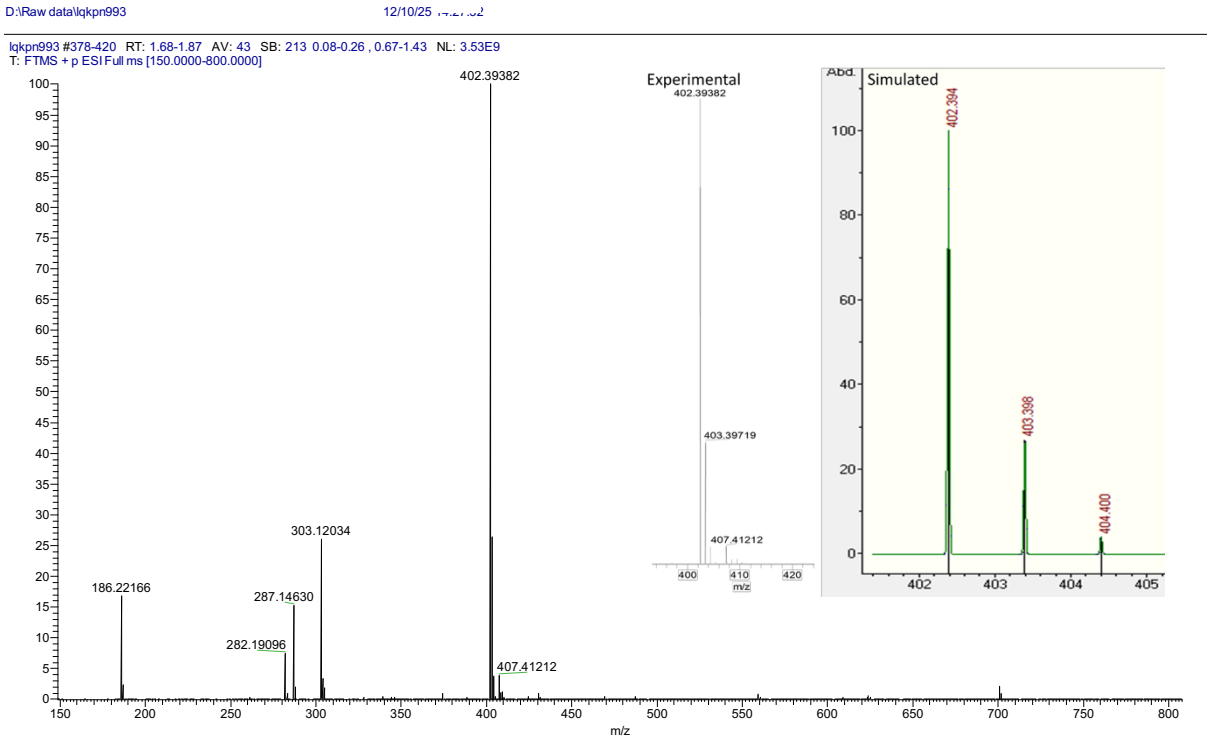

Fig. S26 ESI mass spectrum of (*R*)-**5**. The inset shows the experimental and simulated isotopic patterns of the $[M+H]^+$ ions.

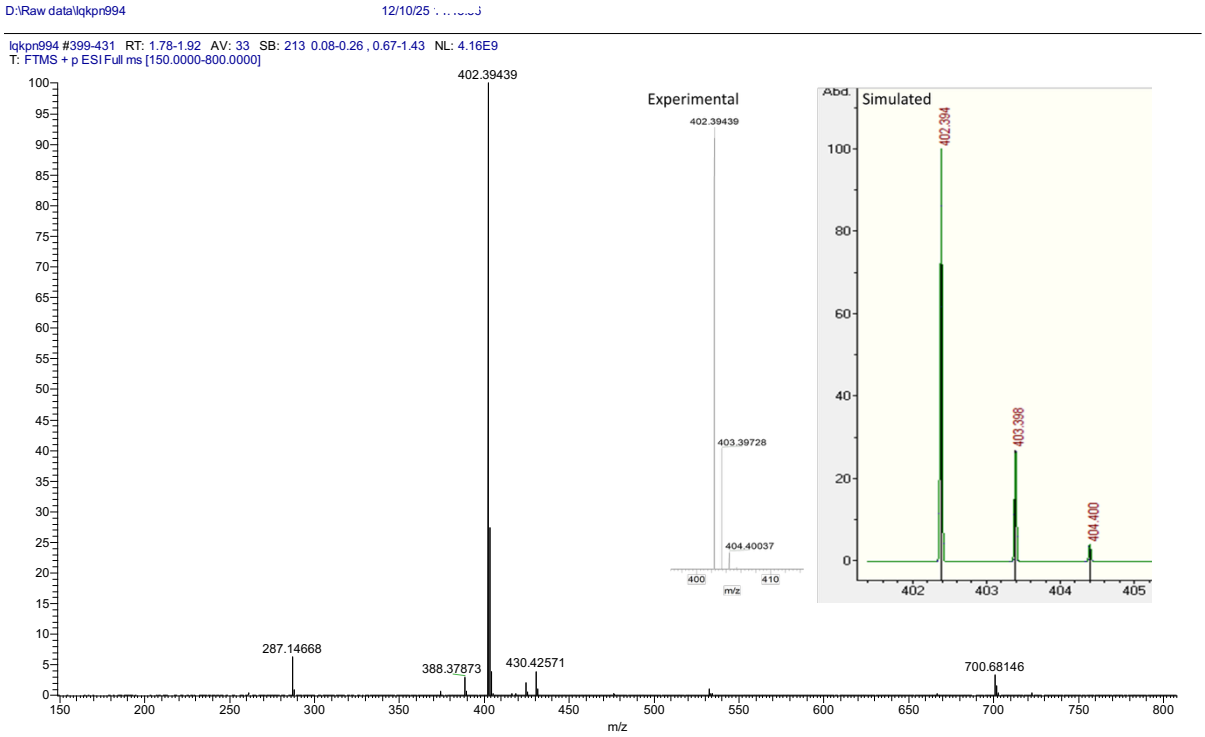

Fig. S27 ESI mass spectrum of (*S*)-**5**. The inset shows the experimental and simulated isotopic patterns of the $[M+H]^+$ ions.

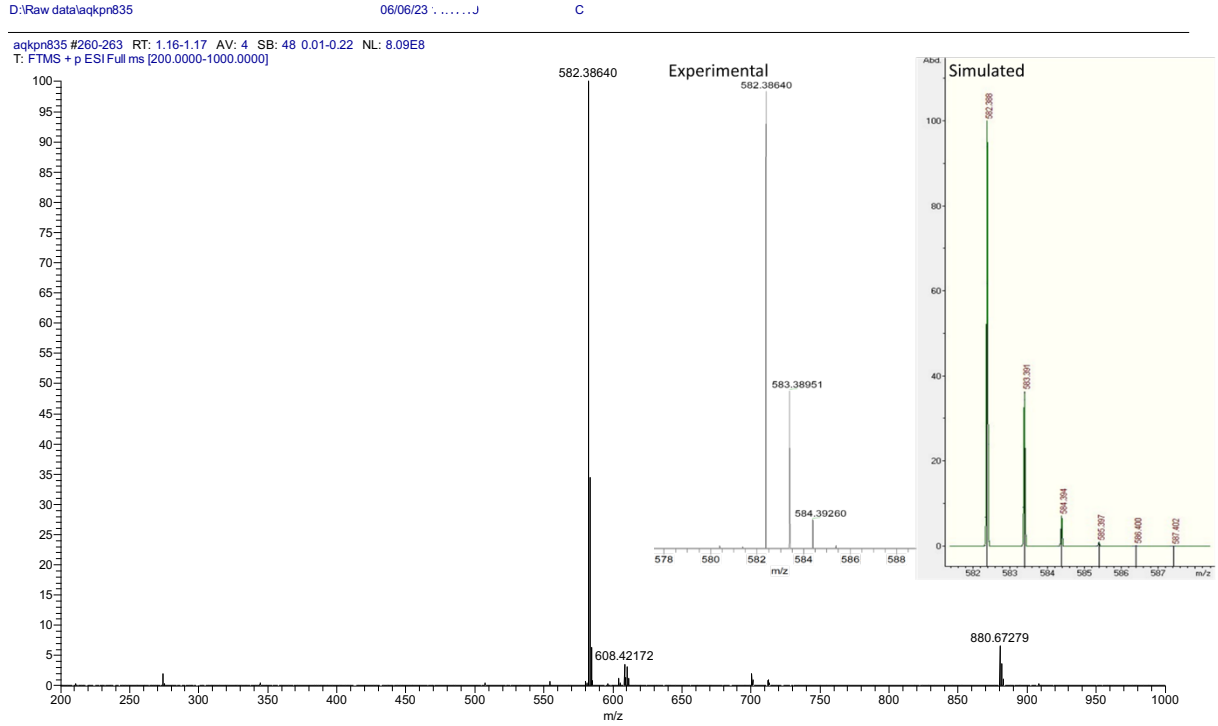

Fig. S28 ESI mass spectrum of (*R*)-**7**. The inset shows the experimental and simulated isotopic patterns of the $[M+H]^+$ ions.

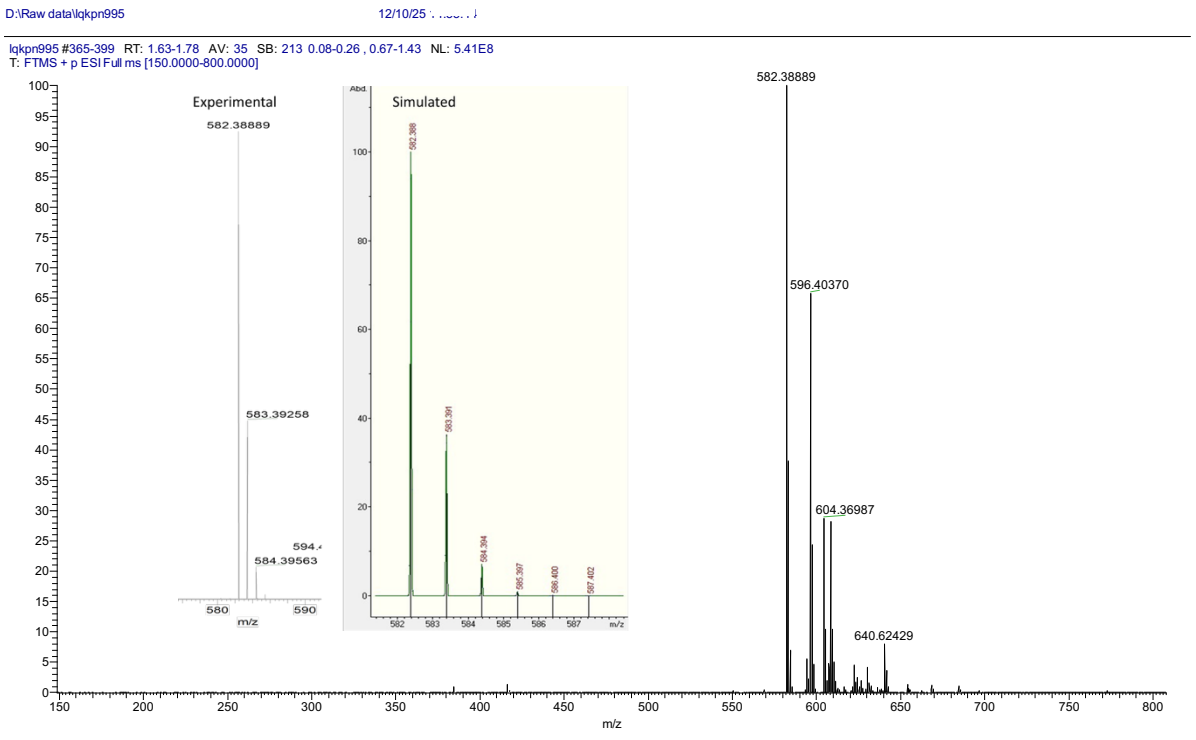

Fig. S29 ESI mass spectrum of (*S*)-**7**. The inset shows the experimental and simulated isotopic patterns of the $[M+H]^+$ ions.

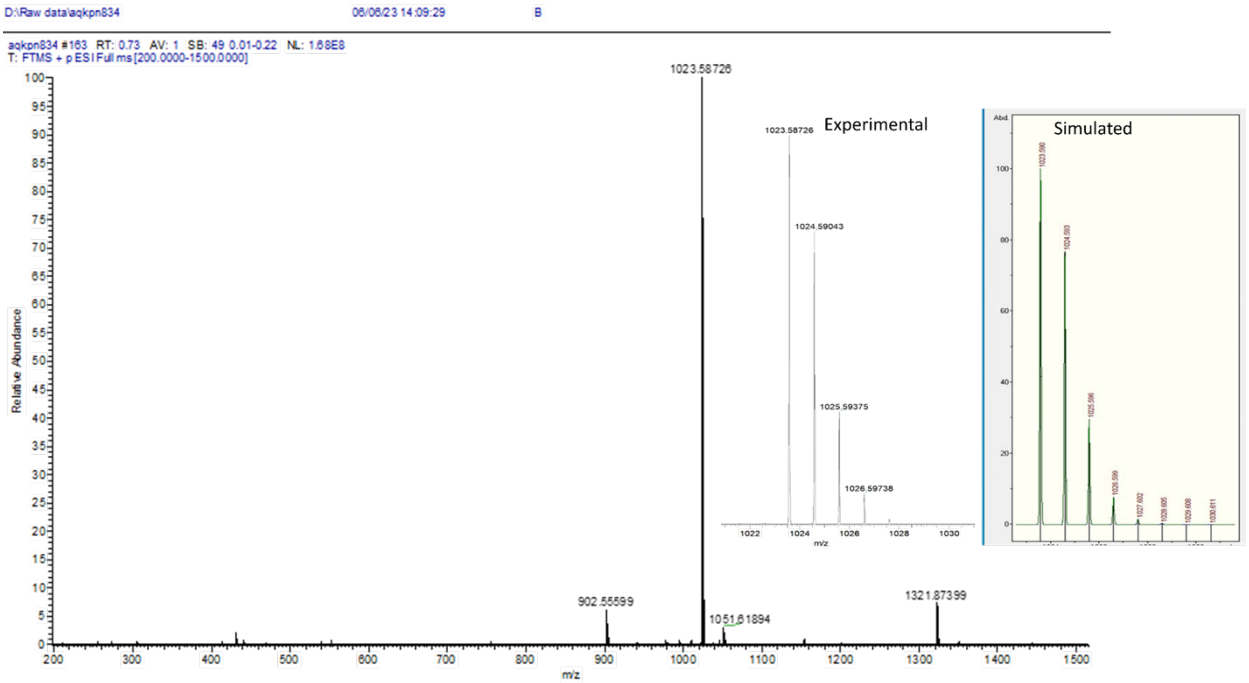

Fig. S30 ESI mass spectrum of (*R*)-**9**. The inset shows the experimental and simulated isotopic patterns of the $[M+H]^+$ ions.

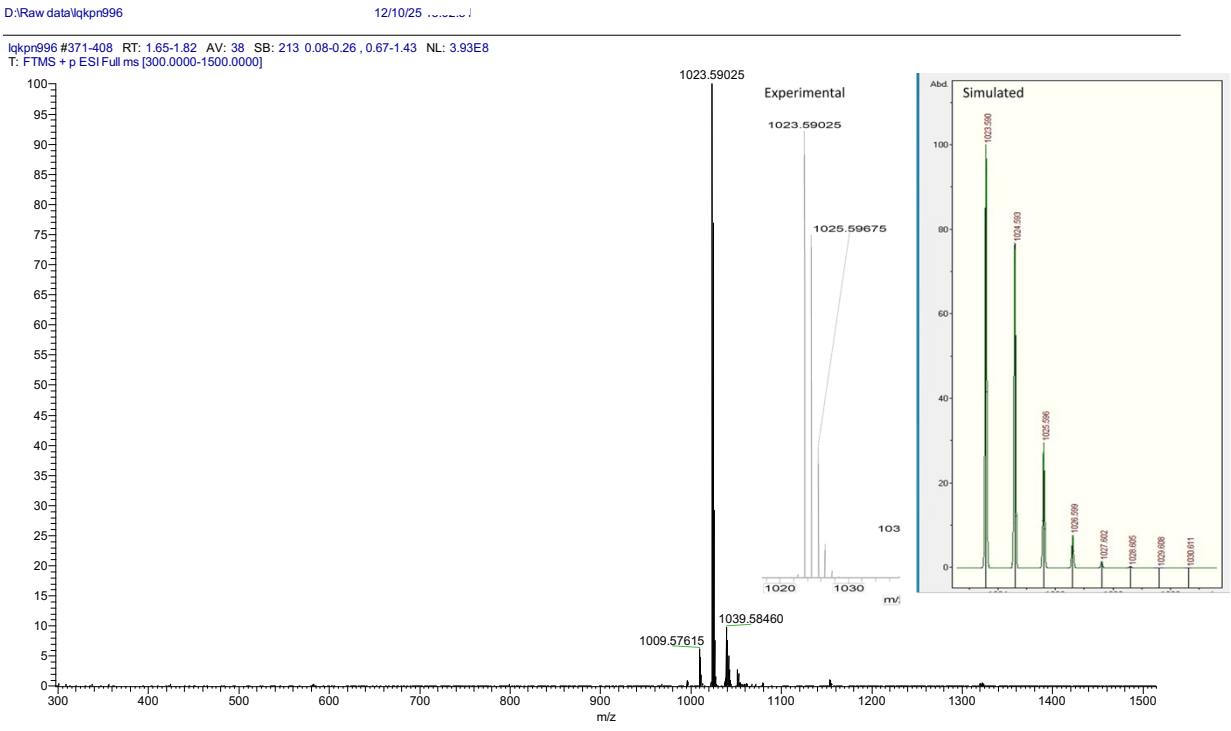

Fig. S31 ESI mass spectrum of (*S*)-**9**. The inset shows the experimental and simulated isotopic patterns of the $[M+H]^+$ ions.